Establishing multiplex *in vivo* assays in a xenograft mouse model of acute leukaemia to correlate preclinical treatment trials with molecular screens

von

Katharina Hunt

Inaugural-Dissertation zur Erlangung der Doktorwürde
der Tierärztlichen Fakultät der Ludwig-Maximilians-Universität
München

Establishing multiplex *in vivo* assays in a xenograft mouse model of acute leukaemia to correlate preclinical treatment trials with molecular screens

von Katharina Hunt

aus Gütersloh

München 2023

Aus dem Veterinärwissenschaftlichen Department der Tierärztlichen Fakultät der Ludwig-Maximilians-Universität München

Lehrstuhl für Molekulare Tierzucht und Biotechnologie

Angefertigt unter der Leitung von: Univ.-Prof. Dr. Eckhard Wolf

Angefertigt am: Helmholtz Munich
Abteilung für Apoptose in hämatopoetischen Stammzellen
Mentorin: Univ.-Prof. Dr. Irmela Jeremias

Gedruckt mit Genehmigung der Tierärztlichen Fakultät
der Ludwig-Maximilians-Universität München

Dekan:	Univ.-Prof. Dr. Reinhard K. Straubinger, Ph.D.
Berichterstatter:	Univ.-Prof. Dr. Eckhard Wolf
Korreferent:	Univ.-Prof. Dr. Johannes Hirschberger

Tag der Promotion: 22. Juli 2023

Teilergebnisse der vorliegenden Arbeit wurden als Poster veröffentlicht in HemaSphere 2022 unter dem Titel: *"P323:Streamlining preclinical in vivo treatment trials by multiplexing genetically labelled PDX models of several patients in a single mouse"* Dieser ist zu finden unter:

https://journals.lww.com/hemasphere/Fulltext/2022/06003/P323__STREAMLINING_PRECLINICAL_IN_VIVO_TREATMENT.223.aspx

Meiner Familie

Coco, Onora, Hope, Willi und Grace

Table of contents

List of Abbreviations

°C	Degrees Celcius
µl	Microliter
ABL1	Abelson murine leukaemia viral oncogene homolog 1
AL	Acute leukaemias
ALL	Acute lymphoblastic leukaemia
AML	Acute myeloid leukaemia
APC	Allophycocyanin
B-ALL	B-lymphoblastic leukemia
BCL2	B-cell lymphoma 2
BCL-XL	B-cell lymphoma-extra large
BCR	Breakpoint Cluster Region Protein
BCS	body conditions score
BLI	Bioluminescence imaging
BM	Bone marrow
CAR-T-cells	Chimeric antigen receptors T-cells
Cas	CRISPR-associated
CDKN2A	Cylin-dependent kinase inhibitor 2A
CDX	Cell-line derived xenograft model
CHOP	Cyclophosphamid, Hdyroxydaunorubicin, Vincristin, Predinisolone
CLL	Chronic lymphatic leukaemia
cm	Centimeter
CNS	Central nervous system
CRISPR	Clustered regularly interspaced short palindromic repeats
CRLF2	Cytokine receptor like factor 2
Cre	Cyclization recombination
D N A	Deoxyribonucleic acid
DKFZ	Deutsches Krebsforschungs Zentrum
DMSO	Dimethylsulfoxid
DNAse	Deoxyribonuclease
DUX4	Double homeobox 4
EBF1	Early b-cell factor 1
eFFLy	Enhanced firefly
eGFP	Enhanced green fluorescent protein
EGFR	Epidermal growth factor
ETV6	ETS Varian Transcription Factor 6
f	Female
FACS	fluorscence activated cell sorting
FBXW7	F-box and wd repeat domain containing 7
FCS	Fetal calf serum

FDA	Food and Drug Administration
FDR	False Discovery Rate
feLV	Feline Leukaemia Virus
FFC	Forward scatter
FISH	Fluorescence in-situ hybridization
FLT3	FMS-like tyrosine kinase 3
Foxn1nu	Athymic nude mice
g	Gramm
GEMM	genetically-engineered mouse model
H-2Kk	Murine histocompatibility antigen
HSC	haematopoietic stem cells
HSP90B1	Heat shock 90 beta family member 1
IGH	Immunoglobulin heavy locus
i.v.	Intravenous
IDH1/2	Isocitrate dehydrogenase
IKFZ	Ikaros family zinc finger 1
IL3	Recombinant humane interleukin-3
indels	Insertions or deletions
INFORM	Individualized Therapy For Relapsed Malignancies in Childhood
iRFP	Near-infrared fluorescent protein
JAK	Janus Kinase
kg	Kilogram
KMT2A	Histon-Lysin-N-Methyltransferase 2A
KRAS	Kirsten rat sarcoma virus
L	Liter
LIC	Leukaemia initiating cells
LSC	Leukemic stem cell
loxP	Locus of x-over, P1
LYL1	Basic Helix-loop-helix family member
m	Male
MAGecK	Model-based Analysis of Genome-wide CRISPR-Cas9 Knockout
mCherry	Monomeric cherry fluorescent protein
MCL1	Induced myeloid leukemia cell differentiation protein
mg	Miligram
min	Minute
ml	Mililiter
MLL	KMT2A rearrangement
MOPP	Mechlorethamine, Vincristine, Procarbazine, Predinosolone
mtagBFP	Monomeric blue fluorescent protein
MTOR	Mechanisitic target of rapamycin
n.s.	not significant
NIBR PDXE	Novartis Institute for Biomedical Research PDX Encyclopedia
NK	Natural killer cell
nm	Nanometer
NOD	Non-obese diabetic
NOTCH1	Neurogenic locus notch homolog protein 1

NSG	NOD.CgPrkdc^{scid} Il2rg^{tm1Wjl}/SzJ
P2RY8	P2R receptor family member 8
p.o.	per os/ oral gavage
PAX5	Paired Box 5
PBX1	Pre-B-cell leukaemia transcription factor
PBMC	Peripheral Blood Mononuclear Cells
PBS	Phosphate buffered saline
PDMR	NCI Patient-Derived Models Repository
PDX	Patient derived xenograft model
PH+	Philadelphia chromosome positive
ProXe	Public Repository of Xenografts
RNA	Ribonucleic acid
ROI	Region of interest
rtPCR	Reverse transcription polymerase chain reaction
RUNX1	Runt related transcription factor 1
s.c.	Subcutan
SCID	Severe combined immunodeficiency
sgRNA	Single guide RNA
SINE	Selective inhibitors of the nuclear export
SPF	Specified pathogen-free
SPL	Spleen
SSC	Side scatter
TAL1	T-cell acute lymphocytic leukaemia protein 1
T-ALL	T- lymphoblastic leukemia
TCF3	Transcription factor 3
TKI	Tyrosine Kinase Inhibitor
TLX1	T cell Leukaemis homebox 1
TLX3	T cell Leukaemis homebox 3
tNGFR	Truncated nerve growth factor receptor
TP53	Tumor Protein 53
XPO1	Exportin 1

List of Figures

List of Tables

1. Literature

1.1. Acute leukaemia in humans

Healthy blood cells arise from a common hematopoietic stem cell in the bone marrow through maturation and differentiation. Acute leukaemia is a malignant disease of the hematopoietic system originating from stem or progenitor cells of the lymphoid or myeloid blood lineage. Leukaemia occurs when an immature or mature cell degenerates and blocks the physiological maturation process of the affected cells. These cells are called lymphoblasts in acute lymphoblastic leukaemia (ALL) and myeloblasts in acute myeloid leukaemia (AML). Hence, the excessive proliferation interferes with the healthy haematopoiesis. (WOLACH & STONE, 2015) (Kompetenznetz Leukämie)

Clinical manifestation involves accumulation of malignant differentiated lymphoid or myeloid cells in the bone marrow, spleen and extra medullary sites such as central nervous system (CNS). Patients develop symptoms within a few weeks and suffer from bone marrow failure, which manifests in anaemia, thrombocytopenia and leukopenia. Further symptoms including fever, weight loss, easy bleeding, dyspnoea and infection have been described; CNS involvement can include facial palsy. In AML CNS symptoms, respiratory distress, skin changes and chloroma are less common. Differential diagnosis of lymphoblastic lymphoma should be considered, since it is not distinguishable from ALL through morphologic or genetic factors. The primary location differs from ALL and occurrence of mass lesions speaks in favour of lymphoblastic lymphoma. (TERWILLIGER & ABDUL-HAY, 2017; BROWN et al., 2020) (Kompetenznet Leukämie)

Acute leukaemia can be diagnosed by haematological cytological examination if more than 20% blasts are present in the blood or bone marrow. In order to identify acute leukaemia, the haemato-pathological examination, which includes cytomorphology, is used and the usage of cytogenetics and molecular cytogenetics, e.g. fluorescence in-situ hybridization (FISH). (DOHNER et al., 2017; BROWN et al., 2020)

The number of globally diagnosed leukaemia increased from 354.5 thousand in 1990 to 518.5 thousand in 2017 (DONG et al., 2020). 6,660 new cases of ALL and 1560 deaths and 20,500 new cases of AML and 11,540 deaths in the United States were reported for 2022 (SIEGEL et al., 2022).

Acute leukaemia is a rare disease and accounts approx. 0.8% of all new cancer cases and accounts 12% of haematological neoplasia in Germany. In Germany, 532 children (<15 years old) as well as 2307 women and 2665 men were diagnosed with acute leukaemia in 2018. The overall five-year survival is approx. 47% for ALL and 25% for AML, for those over 15 years old. The median age of onset in ALL is 26 years in women and 22 years in men. In contrast, AML is a disease that occurs mainly in older people with an average age of 72 years at onset. Men are more likely to develop AML than women. (KIM-WANNER & KRAYWINKEL, 2022)

Standard of care treatment is chemotherapy, both for ALL and AML. Relapse, i.e. myeloid or lymphoid leukaemia cells return after treatment, remains challenging. In AML, 40-50% of junior patients and majority of older patients eventually relapse (BOSE et al., 2017; DOHNER et al., 2017; THOL & GANSER, 2020). In ALL, most of the patients (~85%) respond towards chemotherapy, but a minority relapse (HUNGER & RAETZ, 2020).

1.1.1. Acute lymphoblastic leukaemia (ALL)

ALL is characterised by abnormal, malignant proliferation and differentiation of lymphoid progenitor cells in the bone marrow and blood. In ALL, a number of lymphoid stem cells become lymphoblasts, also known as leukaemia cells. The leukaemia cells block the space for healthy white blood cells and thus suppress the bone marrow, causing the symptoms mentioned above. In advanced stages, infiltration into other organs can occur. (National Cancer Institute)(TERWILLIGER & ABDUL-HAY, 2017).

The World Health Organization classified the ALL into two types: B-lymphoblastic leukaemia/lymphoma and T-lymphoblastic leukaemia/lymphoma (ARBER et al., 2016).

B-ALL is the most common type, classified in B-cell lymphoblastic leukaemia, not otherwise specified and B-cell lymphoblastic leukaemia, with recurrent genetic abnormalities and over 20 subtypes (TERWILLIGER & ABDUL-HAY, 2017; INABA & MULLIGHAN, 2020). For T-ALL, currently two provisional entities are listed, early T-cell precursor lymphoblastic leukaemia and natural killer (NK) cell lymphoblastic leukaemia (ARBER et al., 2016).

Genetic abnormalities associated with T-ALL include mutations of NOTCH1 and FBXW7. The major transcriptional rearrangements in T-ALL are TLX1, TLX3, LYL1, TAL1 and KMT2A. (BROWN et al., 2020)

The diversity of B-ALL can be attributed to chromosomal aneuploidy, rearrangements and point mutations (INABA & MULLIGHAN, 2020).Therefore genetic characterization is important to identify genetic and chromosomal abnormalities, which can be crucial in terms of therapy (BROWN et al., 2020).

Common chromosomal abnormalities in B-ALL are aneuploidy, which refers to the deviation of chromosomes form the original set (HASSOLD & HUNT, 2001; INABA & MULLIGHAN, 2020). High hyperdiploidy (>50 chromosomes) can be found in up to 30% of childhood ALL, while low hypodiploidy (31-39 chromosomes) occurs in only 1% of paediatric ALL and around 10% of adult ALL. Furthermore, near haploidy (24-30 chromosomes) is detectable in 2% of childhood ALL. (INABA & MULLIGHAN, 2020)

Chromosomal rearrangements, such as translocations mainly occur in ALL. The translocation t(21;21)(p13;q22) is the most frequent one in childhood ALL. In infants, the rearrangement of KMT2A (MLL) t(4;11) (q21;q23) is the most frequent one. The t(9;22) (q34;q11.2) translocation leads to the formation of the Philadelphia chromosome that results in the BCR::ABL1 fusion protein. These can be found in 20-25% of adults harbouring ALL. (INABA & MULLIGHAN, 2020)

Chromosomal predispositions such as Down syndrome are associated with higher risk to develop acute lymphoblastic leukaemia, both B-ALL and T-ALL. Familial genetic predispositions are rare and can include *TP53* germline mutations, *PAX5* mutations, *ETV6* variants, low hypodiploid B-ALL and high hyperdiploid ALL. Causes extend into the prenatal period, such as KMT2A-rearranged and ETV6-RUNX1 ALL. (INABA & MULLIGHAN, 2020)

In a study, Mullighan detected EBF1, PAX5 and IKFZ1 as the most frequent mutations, which are all involved in the development of b-cells. 31.7% of cases revealed a mutated PAX5 gene (MULLIGHAN et al., 2007). PAX5 plays a role in b-lineage formation (NUTT et al., 1999) and EBF1 is needed to express PAX5 (LIAO, 2009). IKFZ1 mutations are present in 15-20% of paediatric ALL and linked with poor prognosis (BROWN et al., 2020).

The therapeutic scheme of patients diagnosed with ALL includes induction, consolidation and maintenance therapy over a period of approximately 2 to 2.5 years.

During induction therapy, patients receive a glucocorticoid and a combination of two cytostatic drugs (vincristine and asparaginase) over a period of 4 weeks. The aim is to reduce tumour burden by removing leukemic cells from the bone marrow. This results in a complete remission, i.e. the disappearance of all signs of cancer, in 98% of patients. During consolidation therapy, patients receive the cytostatic agents' cyclophosphamide, cytarabine and asparaginase. Here, remaining leukemic cells should be eliminated. Furthermore, cranial radiation, and/or intrathecal therapy is performed, since lymphatic blasts can also affect the brain, where chemotherapy is not effective. (BROWN et al., 2020; INABA & MULLIGHAN, 2020)

To avoid relapse, maintenance therapy is crucial and includes mercaptopurine and methotrexate. Sometimes, vincristine and steroids are added. Allogeneic stem cell transplantation is considered in high risk patients (INABA & MULLIGHAN, 2020).

Newer approaches include targeted therapies (see 1.4.2), immunotherapy and the combination of chemotherapy with these.

1.2. Acute leukaemia in animals

Acute leukaemia's play a role in pets and livestock, too. Lymphoid cancers are the most commonly diagnosed malignancies in dogs. However, the overall incidence in dogs is not known, but golden retrievers seem to be overrepresented as patients with ALL. Similar to humans, different forms of lymphoid leukaemia can be distinguished, e.g. CLL, T-zone lymphomas, non-Hodgkin lymphoma and ALL. Canine acute lymphoblastic leukaemia is a progressive and chemo-resistant cancer with a very poor outcome. Cytology and immunophenotyping are used for the diagnosis. Notably, there is no standard scheme for the diagnosis of canine ALL. The diagnosis of canine ALL ranges from 30-20% blasts in bone marrow with either marked lymphoblastic leucocytosis including thrombocytopenia and anaemia or the presence of circulating blasts and cytopenia's in one or more lineages. Immunophenotypic analysis is also used. Here, detection for CD34 is examined. Thoracic radiography and ultrasound examinations are also performed. The dogs present with lethargy, inappetence, peripheral lymphadenopathy and cranial abdominal organomegaly. Therapy follows the CHOP protocol, which includes cyclophosphamide, doxorubicin, vincristine and prednisolone. There are also other treatment schemes, e.g. MOPP – mechlorethamine, vincristine, procarbazine and prednisolone. However, survival rates are poor with a median of 55 days. (BENNETT et al., 2017; ATHERTON & MASON, 2022)

Acute myeloid leukaemia's also occur in dogs and are similar to canine ALL in terms of clinical sings and diagnostic strategies. In particular, organomegaly and lymphadenopathy are prominent in canine AML. (EPPERLY et al., 2018)

There are few studies of feline ALL, but the outcome is as poor as in canine ALL. Clinical signs are anorexia and lethargy and therapy is similar to canine ALL (TOMIYASU et al., 2018). In cats, feline leukaemia is often associated with feline leukaemia virus (FeLV), but not every cat diagnosed with FeLV develops a leukaemia. FeLV is an infectious disease that occurs worldwide. Transmission is possible through close contact, catfights, or vertically from queen to kitten. FeLV first occurs in local lymphoid tissues and then spreads into periphery via lymphocytes and monocytes. This is called primary viremia. Primary viremia can affect the bone marrow. After infection of the bone marrow, FeLV is detectable in blood with FeLV-infected leukocytes and platelets. Infection can be divided into three stages; progressive infection with viremia and shorter survival time; regressive infection, where the immune response is present but not strong enough to completely kill the virus; and abortive infection, when cats tested negative but the presence of antibodies is characteristic. FeLV can be

diagnosed by point-of-care screening test and the presence of FeLV p27antigen in serum, plasma or blood. In addition, PCR tests are used, as well as saliva swab test for large groups, e.g. in animal shelters. Prevention can be done with vaccination, which is recommended for kittens after 8 weeks, and a second vaccination after another 3-4 weeks. A booster vaccination is recommended every 2 years. (HOFMANN-LEHMANN & HARTMANN, 2020; LITTLE et al., 2020)

In cattle, enzootic bovine leucosis, caused by the bovine leukaemia virus, is a fatal disease associated with a decline in milk production and life expectancy, leading to economic losses for farms. It has been eradicated in over 20 countries (BARTLETT et al., 2020). Other forms of leukaemia, such as AML, have been diagnosed in cattle, too (MAEZAWA et al., 2021). Since 1999, Germany is declared as free of bovine leucosis, but the disease is notifiable according to the Cattle Health Surveillance Ordinance (Rindergesundheits-Überwachungs-Verordnung, BGBl. II Nr. 334/2013).

1.3. The use of animals in cancer research

According to the German Federal Institute for Risk Assessment, in 2020 around 1.9 million animals were used in animal experiments in Germany. Mice were the most represented species and approx. 48.1% of the animals were genetically engineered. For cancer research, 98,412 animals were used for basic research and 105,704 animals for translational research (BfR, 2021). Animals are protected by the German Animal Welfare Act, the German Animal Welfare Experimental Ordinance and the EU directive 2010/63 EU. Each experiment is subject to an ethical consideration and must be designed in such way that no unjustified pain, suffering or harm is inflicted on the animal.

In 1959, Russell and Burch published the 3R concept to conduct humane animal research, consisting of the principles reduction (minimising the number of animals used for a scientific objective), refinement (minimising pain, suffering and distress), and replacement (avoiding animal trials if a suitable other technique exists). (RUSSELL & BURCH, 1959)

Animal models in cancer research are well established. Especially mouse models are used as a popular tool. The advantages of using mice includes small size, high reproduction rate and low costs in housing (CHEON & ORSULIC, 2011). Additionally, mice can be genetically engineered, which was first described in the 1980s and revolutionized the tumour biology studies (BRINSTER et al., 1982).

Other animal models include e.g. dogs, which bear a close resemblance to the human genome. The anatomy, physiology and genetic characteristics of pigs are also similar to humans. Non-human primates convince due to similarity in physiology, immunity and many other characteristics. However, compared to small animal models, the experiments are more complex due to higher costs and ethical considerations. Further animal models used in cancer research include zebrafish, rats, tree shrew, fruit flies and many more. (LI et al., 2021)

1.3.1. The patient-derived xenograft mouse model

A patient-derived xenograft mouse model is generated when tissue of a human patient is transplanted into a mouse. (SIOLAS & HANNON, 2013)

The first patient-derived xenograft model was described in 1969 when Rygaard and Povlsen implanted a piece of an adenocarcinoma of a 74 year old patient into *Foxn1*^{nu} mice subcutaneously. The tumour grew as local nodules but did not metastasize (RYGAARD & POVLSEN, 1969). Today, this method is named ectopic implantation, since the implantation locus differs from the origin. In 1982, Wang and

Sordat were the first who described the orthotopic transplantation. They injected colon cancer cells from a patient into the large intestine of nude mice and tumour engraftment and metastasis were observed (WANG et al., 1982). Later on, the models were optimized using advanced immunodeficient mice in order to increase the engraftment rate. Among other mice strains, the NOD-*scid IL2Rgamma* ^{null} (NSG) strain, which lacks in B-, T-, NK-cells and several cytokine pathways, is often used for the engraftment of hematopoietic stem cells in mice (SHULTZ et al., 2005). In addition, humanized mouse models are increasingly being used. Here, models were developed including haematopoietic stem cells (HSC) and peripheral blood mononuclear cells (PBMC) (YONG et al., 2018).

For some entities, it is more difficult to establish PDX models, e.g. hormone-positive breast cancers with an engraftment capacity of 13%; while, for non-small cell lung cancer, a transplant capacity of 90 % has been reported in NOD-*scid* mice (CHO, 2020). In ALL establishment rates vary and some studies report an engraftment capacity of 100% (LOCK et al., 2002), whereas other studies show engraftment capacities of 44% (AGLIANO et al., 2008).

Orthotopic PDX models mimic the histopathological structure of the primary tumour (KUWATA et al., 2019). Furthermore, the histology of PDX samples after serial transplantation is consistent to the primary tumour, compared to cell-line derived xenografts (CDX) (SCHUELER et al., 2018; KUWATA et al., 2019).

The disadvantages of PDX models include long engraftment periods, ranging from weeks to months, and an engraftment capacity that varies depending on the type of tumour. Several studies have shown, that murine stroma replace the human tumour stroma. Furthermore, immunodeficient mouse strains are used, since other strains would reject the xenografts, which makes them unattractive for the study of immunological processes and the development of immune-based therapeutics or vaccines. (SIOLAS & HANNON, 2013; HIDALGO et al., 2014; SAJJAD et al., 2021)

1.3.2. Patient-derived xenograft mouse models in preclinical cancer research

The development of therapies requires intensive preclinical testing and patient-derived xenograft models provide an optimal platform (GAO et al., 2015; TOWNSEND et al., 2016).

Several researchers already observed the success rate in PDX models are correlating well with the clinics. For example, the EGFR inhibitor cetuximab was tested in over 40 colorectal PDX models and showed a response rate of 10.6%, which was also seen for patients in the clinics (BERTOTTI et al., 2011). Additionally, mTOR inhibitors were tested in PDX models of *KRAS*-mutant colorectal cancer, predicting poor efficacy in line with what was seen in the clinics. Sirolimus was tested in PDX models of renal cell carcinoma and response was similar observed in the clinics (HIDALGO et al., 2014). These are just few examples, which proved, that PDX models are a helpful and reliable tool to identify novel therapies for the improvement of cancer treatment. On the other hand, about 85% of preclinical compounds fail in clinical trials and do not receive regulatory approval. (MAK et al., 2014; GAO et al., 2015).

Meanwhile, several consortia with large PDX cohorts have been created and characterised to conduct large-scale preclinical drug testing, such as EuroPDX, Public Repository of Xenografts (ProXe), NCI Patient-Derived Models Repository (PDMR), Novartis Institute for Biomedical Research PDX Encyclopedia (NIBR PDXE) and The Jackson Laboratory PDX cohort. (CHO, 2020)

1.3.3. Patient-derived xenograft mouse models in acute leukaemia

As for other tumour entities, also ALL was established as orthotopic, systemic xenograft models (KAMEL-REID et al., 1989; LOCK et al., 2002; LIEM et al., 2004; TERZIYSKA et al., 2012). The leukemic cells infiltrate the bone marrow, spleen and liver, and eventually other organs like CNS, as well as splenomegaly was observed, similar as in patients, indicating that the xenograft mouse model is able to recapitulate the human leukaemia in mice (LOCK et al., 2002).

Here, patients' primary leukemic cells gained from bone marrow aspiration or peripheral blood are transplanted into the tail vein or femur of severely immunocompromised mice. At first, *scid* mice were used (KAMEL-REID et al., 1989; CESANO et al., 1992), however, Shultz et al generated an even more immunocompromised mouse strain the NSG mouse. Here, engraftment of human leukemic cells evolved in a higher success rate compared to other immunocompromised strains such as NOD/LtSz-*Prkdc*^{scid} and NOD.Cg-*Prkdc*^{scid}*B2m*^{tm1Unc} (SHULTZ et al., 2005; AGLIANO et al., 2008).

Successful engraftment is monitored by analysis of chimerism in peripheral blood, bone marrow and eventually other organs like spleen or liver (NIJMEIJER et al., 2001; SHULTZ et al., 2005; AGLIANO et al., 2008). Apart from initial engraftment, the cells can also be re-isolated from the murine organs and re-injected into next recipient mice to establish robust PDX models and to multiply rare primary patient material (BORGMANN et al., 2000; LIEM et al., 2004; TERZIYSKA et al., 2012; TOWNSEND et al., 2016).

This model has been used to characterize leukemic stem cells (BONNET & DICK, 1997; WANG & DICK, 2005; LE VISEUR et al., 2008), in preclinical treatment trials to test chemotherapeutics, such as vincristine (LOCK et al., 2002; LIEM et al., 2004), as well as targeted therapies (GAO et al., 2015; TOWNSEND et al., 2016).

In order to intensify the study of the leukemic disease *in vivo*, genetic engineering of PDX models was established in the hosting laboratory. PDX cells can be lentivirally transduced to express a plethora of diverse transgenes. Fluorochrome expression enables enrichment of transgenic cells by fluorescence activated cell sorting (TERZIYSKA et al., 2012; EBINGER et al., 2016); expression of luciferase facilitates to monitor the growth of the leukemic cells *in vivo* (CASTRO ALVES et al., 2012; TERZIYSKA et al., 2012; VICK et al., 2015); fluorochromes, barcodes and tags enable the distinction of single cell clones over time (ZELLER et al., 2022); distinct fluorochrome combinations enable competitive *in vivo* assays (LIU et al., 2020; WIRTH et al., 2022); expression of Cre and loxP sites enable inducible knock out screens (CARLET et al., 2021); and expression of Cas9 and sgRNA libraries enable CRISPR/Cas9 dropout screens to identifying novel targets (GHALANDARY et al., 2022; WIRTH et al., 2022).

Taken together, the xenograft mouse model is a suitable tool to study acute leukaemia *in vivo* and to identify novel targets and treatment options.

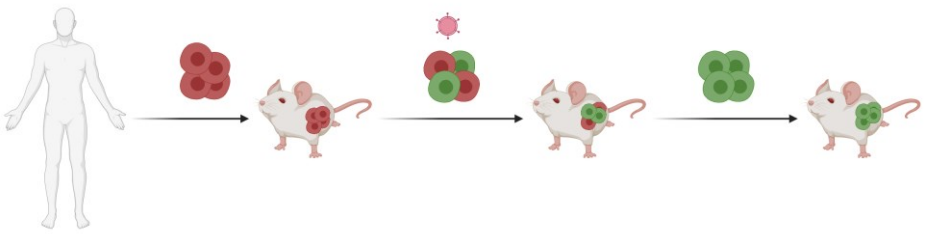

Figure 1. The genetically engineered patient-derived xenograft model

Primary patient material transplanted into NSG mice (P0). After re-isolating cells, PDX cells are genetically engineered by lentiviral transduction and injected into next recipient mice (P1). Afterwards genetically engineered leukaemia cells are serial transplanted (P2-PX). Engraftment success is dependent on the mouse strain and the primary patient material.

1.3.4. Competitive transplantation assays to allow multiplex *in vivo* assays

Competitive transplantation assays are commonly used to evaluate functionality of hematopoietic stem cells (HSC), e.g. the capacity to engraft in recipient mice. Here, HSCs from different origins, e.g. isolated from different mouse strains (HARRISON, 1980) or different human organs (ROSLER et al., 2000), or HSC marked with e.g. genetic barcodes (BRUGMAN et al., 2015), are mixed and injected into recipient mice. The functionality and quantity of HSCs derived from different populations are compared over time. This method is used to evaluate the ability of differentiation and self-renewal of HSCs. Analysing differentiation of the populations is possible by detecting surface markers using flow cytometry (SZILVASSY et al., 1990; KWARTENG & HEINONEN, 2016). In leukaemia research, similar assays are used to investigate functionality of leukemic stem cells (LSC) or leukaemia initiating (LIC) cells (CORNILS et al., 2014; MAETZIG et al., 2017).

1.3.4.1. Genetic labelling of cells to enable competitive *in vivo* assays

To track and discriminate single cells over time, cells can be lentivirally transduced with red, blue and green fluorescent proteins (WEBER et al., 2011). These cells can be detected and discriminated in flow cytometry by their individual colour, respectively (MAETZIG et al., 2018). Red blue green marking was initially generated to reveal clonal tumorigenesis (WEBER et al., 2011) but can also be used for competitive *in vivo* trials in leukaemia research (CARLET et al., 2021; GHALANDARY et al., 2022; WIRTH et al., 2022; ZELLER et al., 2022). Furthermore, cells can be marked with tags, for instance tNGFR (truncated nerve growth factor receptor).

Another method to facilitate competitive *in vivo* transplantation assays is the labelling of cells with individual genetic barcodes. Here, cells are transduced with a library consisting of huge numbers of individual short genetic stretches, injected into mice and can be later quantified by high throughput sequencing. Studies labelling ALL and AML cells with barcodes have been successfully conducted. These studies investigated which cells engraft and gain an advantage or disadvantage over time, or show response towards therapy (ELDER et al., 2017; BRAMLETT et al., 2020; ZELLER et al., 2022).

To my knowledge and until today, competitive transplantation assays with human leukaemia cells were always restricted to cells originating from the same donor. As pioneering work performed in the hosting laboratory, Wirth and colleagues competitively transplanted fluorochrome labelled ALL PDX cells of five different patients into recipient mice, which were then treated with the BCL2 inhibitor venetoclax (WIRTH et al., 2022).

In the following study this competitive *in vivo* transplantation assay of different patient cells is termed "multiplex *in vivo* assay".

1.4.Precision medicine in oncology

Precision oncology includes the molecular characterization of the patients' tumour and addressing these characteristics with targeting therapies (SAWYERS, 2004; ASHLEY, 2016; LASSEN et al., 2021). Various definitions exist for precision medicine. In the following, I define the term "precision medicine" as an approach in which an individual patient receives a tailored treatment. Nowadays, there are various concepts to address this aim.

1.4.1. Characterisation of patient's tumours for precision medicine

1.4.1.1. Molecular analysis to predict drug response

Independent of leukaemia, most recurrent mutations occur with a frequency of less than 20% across cancer types, making it difficult to assign patients the treatment they need (LAWRENCE et al., 2014). The integration of genomics is widespread and tailored to genetic aberration. Several groups and institutes have started and conducted clinical trials to learn if results from sequencing approaches can predict effective drugs.

For instance, "INFORM" (Individualized Therapy For Relapsed Malignancies in Childhood) is a precision medicine study for children with high-risk relapsed/refractory malignancies, which aims to identify therapeutic targets on an individualised basis. INFORM characterizes primary tumour samples on a molecular basis including whole exome sequencing, whole genome sequencing, RNA sequencing and a genome wide assessment of DNA methylations. Furthermore, they defined a list of 372 targets and over 800 targeting drugs, to link genomic hits with targeted therapies. The idea is using multi-omics as a biomarker, and defining suitable drugs for individualised cancer therapy. (WORST et al., 2016; VAN TILBURG et al., 2021)

Further precision medicine studies with similar concepts across continents are: NCI MATCH and the pediatric version Pediatric MATCH (Molecular Analysis for Therapy Choice) of the National Cancer Institute in the United States (ALLEN et al., 2017; COYNE et al., 2017); the ZERO Childhood cancer program in Australia (WONG et al., 2020); The European Proof-of-Concept Therapeutic Stratification Trial of Molecular Anomalies in Relapse or Refractory Tumors in Children (AcSé-ESMART) which is guided by a European academic consortium (FORREST et al., 2018) and many more existing.

1.4.1.2. *Ex vivo* approach to predict drug response

A second strategy in personalised medicine is to combine molecular and descriptive data sets, such as whole-exome sequencing and RNA sequencing, with *ex vivo* treatment trials in order to assign patients to tailored therapies. For *ex vivo* studies, patient material is treated with drug libraries which often include conventional chemotherapeutics as well as novel compounds. Patient samples and drugs are plated *ex vivo* and after a define period of time, usually 72 hours, drug response is evaluated. Here, a link between the mutational status and *ex vivo* drug sensitivity was seen (TYNER et al., 2018; MALANI et al., 2022).

1.4.1.3. Using mice in co-clinical trials for precision medicine

Other approaches include mouse models to predict drug response, such as co-clinical trials, also referred to as avatars. Here, PDX models (see 1.3.1) are generated from primary material of patients who are currently in the clinics. Drugs and drug combinations are tested in mice injected with individual PDX cells, and suggestions for individualised therapy is made on the basis of these results. Often this approach has its limitations due to lack of engraftment and time required (HIDALGO et al., 2014).

To circumcise above listed limitations, genetically-engineered mouse models (GEMMs) are also used in co-clinical trials. Since establishment of a xenograft model takes time, large cohorts of mouse models are characterized and if the mutation profiles are similar, they are matched to the patients in the clinics. Preclinical trials are then carried out and suggestions for tailored treatments are made (VASCIAVEO et al., 2022).

In addition, the integration of *ex vivo* drug testing and preclinical *in vivo* trials using PDX samples in combination with genomics and transcriptomics have been described, too (LAU et al., 2022).

1.4.1.4. Using CRISPR/Cas9 dropout screens to identify cancer vulnerabilities and predict drug response

CRISPR (clustered regularly interspaced short palindromic repeats)/Cas (CRISPR-associated) describes a molecular method to cut and change the DNA, which has been evolved in bacterial and archaea immune defence systems. The technology enables the insertion, deletion or knocking out of genes (DOUDNA & CHARPENTIER, 2014).

CRISPR/Cas9 screens have been frequently used to identify cancer vulnerabilities (SHALEM et al., 2014; BEHAN et al., 2019); however, most of the screens have been performed in cell lines and *in vitro* (DEMPSTER et al., 2019). Finding a biomarker to identify candidate drug targets remains challenging and was mainly performed in cell lines (MARCOTTE et al., 2016; BEHAN et al., 2019; GONÇALVES et al., 2020). For leukaemia, only a few CRISPR/Cas9 screens in PDX were recently published (BAHRAMI et al., 2019; GHALANDARY et al., 2022; WIRTH et al., 2022). Until today, this method is not used for precision medicine, but a high potential of CRISPR/Cas9 screens for precision medicine is given, since it enables to identify individual cancer vulnerabilities as described in the studies of Ghalandary and Wirth.

1.4.2. Targeted therapies

Characterisation of patients enables assignment towards targeted therapies. Conventional chemotherapy addresses not only malignant cells, but also healthy cells. Therefore, patients suffer from severe side effects (BAGNYUKOVA et al., 2010).

In addition, relapses remain a major challenge and novel therapeutic options are needed (see 1.1). Technical advances in sequencing are uncovering more and more molecular details to improve treatment. In this context, targeting therapies are being use. There are various definitions of targeted therapies, but "for many scientists and oncologists, targeted therapy is defined as a drug with a focused mechanism that specifically acts on a well-defined target or biologic pathway that, when inactivated, causes regression or destruction of the malignant process" (ROSS et al., 2004).
In the present study, I define "targeted therapies" as a specific therapy which inhibits a defined targeted protein with high specificity.

In 2021, 89 small molecules were approved in the USA and China to treat cancers (ZHONG et al., 2021), whereas only a few are approved for leukaemia. Currently, only 31 targeted drugs are listed to be FDA approved for leukaemia's, but only five of them are available for ALL. In the following, the approved targeted therapies for acute leukaemia's are listed.

1.4.2.1. Kinase Inhibitors

Especially kinase inhibitors are overrepresented and 62 out of 89 approved inhibitors are kinase inhibitors (ROSKOSKI, 2021). Kinase inhibitors can be divided into three main groups: receptor tyrosine kinase inhibitors (TKI), non-receptor TKI, and serine/threonine kinase inhibitors. First generation FLT3 inhibitors such as midostaurin showed improvement in overall survival if combined with conventional chemotherapy in AML patients and gained FDA approval in 2017. One year later, the second generation FLT3 inhibitor gilteritinib was approved by the FDA for relapsed/refractory FLT3 mutated AML, which is more selective towards FLT3 (DÖHNER et al., 2021).

Depending on genetic and chromosomal alterations, ALL patients receive specific therapy. For instance, patients with Ph-positive ALL receiving imatinib, a tyrosine kinase inhibitor targeting

BCR::ABL, which was approved by the FDA in 2001, in combination with chemotherapy showed complete remission in 90% to 95%. In September 2022, a second-generation tyrosine kinase inhibitor dasatinib received FDA approval for ALL. Currently, clinical trials with further second generation tyrosine kinase inhibitors, such as nilotinib, targeting BCR::ABL, are ongoing and under investigation. In Ph-like ALLs, clinical trials investigate the effect of ruxolitinib, a JAK-inhibitor, compared to TKIs (SALVARIS & FEDELE, 2021).

1.4.2.2. IDH2/1 and hedgehog pathway inhibitors

IDH2/1 inhibitors, e.g. ivosidenib and enasidenib are FDA approved for AML patient in combination with chemotherapy. Additionally, clinical trials currently investigate the combination of IDH inhibitors with venetoclax, an inhibitor of the anti-apoptotic protein BCL2 (SHORT et al., 2020).

Among these, the hedgehog pathway inhibitor glasdegib is since 2018 FDA approved in combination with low dose cytarabine for AML patients older than 75 years old, after the successful clinical trial BRIGHT AML 1003 (NCT01546038) (HEUSER et al., 2021).

1.4.2.3. BH3 mimetics

Anti-apoptotic proteins are well known to be overexpressed in AML and ALL, and venetoclax was approved by the FDA in combination with low dose cytarabine, azacitidine or decitabine for patients with AML. On the other Hand, treatment with venetoclax results in resistance and upregulation of *MCL1*. Venetoclax is under clinical investigation for ALL in combination with the BCL-XL inhibitor navitoclax. (SHORT et al., 2020)

1.4.2.4. Immunotherapeutics

T-cell-based therapies, as for example CAR-T cells (chimeric antigen receptors), and antibody therapies are increasingly being used for ALL patients. In 2017, tisagenlecleucel, an anti-CD19 CAR-T cell, received FDA approval for patients up to age 25 with B-cell precursor that is fractory or in second or late relapse, after a study demonstrating an overall survival of 81% in three months. (SALVARIS & FEDELE, 2021)

Further novel therapies include antibody-drug conjugates, e.g. inotuzumab ozogamicin, which showed promising results in clinical trials and was approved in 2017 for refractory and relapsed B-ALL (FDA, 2017). In addition, the bispecific monoclonal antibody blinatumomab was approved for relapsed and refractory B-cell precursor ALL (FDA, 2014). Rituximab, a CD-20 monoclonal antibody, is gaining importance and showed survival improvement for ALL patients under 60 years old (SALVARIS & FEDELE, 2021).

1.4.3. Compounds used for preclinical trials

1.4.3.1. Venetoclax (ABT-199) to target BCL2

Venetoclax is a BCL2 homology domain 3 (*BH3)* mimetic and has the ability to kill cells by apoptosis induction “in a strictly BAX/BAK dependent manner” (ROBERTS et al., 2021; SALAH et al., 2021). Venetoclax is a selective inhibitor and has a >100-fold selectivity for *BCL2* over *BCL-XL* and *BCL-w* and >1000-fold activity for *MCL1* (ROBERTS et al., 2021; SALAH et al., 2021). *BCL2* is known to be

overexpressed in haematological malignancies and plays an important role in the regulation of apoptosis (COUSTAN-SMITH et al., 1996; ROBERTSON et al., 1996; ROBERTS et al., 2021).
The inhibitor binds to the groove of BCL2 proteins, thereby represses the BCL2 activity, and restores apoptotic processed in tumour cells (NIH.gov). Blocking BCL2 restores the signalling cascade that causes cancer cells to destroy themselves (AbbVie Inc.). The doses of 100 mg/kg oral five times per week showed efficacy in preclinical trials and therefore was used in the present study (SOUERS et al., 2013). Preclinical trials demonstrated that mice bearing chronic and acute myeloid, as well as acute lymphoblastic leukaemia showed a response towards venetoclax treatment (SOUERS et al., 2013; PAN et al., 2014; WIRTH et al., 2022). The inhibitor is FDA approved for chronic myeloid leukaemia since 2016 and for AML in combination with cytarabine since 2020 (FDA, 2020), and to date over 190 clinical trials are listed for leukaemia (ClinicalTrials.gov). Human AML patients receive up to 600mg oral once a day (Venclexta.com).

1.4.3.2. S63845 to target MCL1

S63845 binds to human MCL1, but shows no substantial binding to *BCL2* or *BCLXL* (KOTSCHY et al., 2016). Similar to other BH3 mimetics, S63845 binds to the BH3- binding groove (KOTSCHY et al., 2016). *MCL1* is known to be highly expressed in haematological malignancies (GORES & KAUFMANN, 2012; WANG et al., 2021). In a mouse model of ALL it was demonstrated that *MCL1* is required for survival in ALL (KOSS et al., 2013). *MCL1* is not only essential for AML but also for, breast cancers, T cell lymphoma, non-small-cell lung carcinoma and multiple myeloma (WANG et al., 2021).
The Inhibitor showed activity in AML cell lines with IC50 ranging from 4 to 233nM. S63845 was already successfully used in haematological malignancies, as well as in the hosting laboratory *in vitro* and *in vivo*. The published concentration of 25mg/kg intravenously, twice a week was administrated. (KOTSCHY et al., 2016; CARLET et al., 2021)

1.4.3.3. Eltanexor (KPT-8602) to target XPO1

Eltanexor is a XPO1 inhibitor and restores the nuclear localization, function of tumour suppressing proteins and induces apoptosis in tumour cells (CAMUS et al., 2017). *XPO1* is an important export factor, which conducts the transport of proteins from the nucleus to the cytoplasm (CAMUS et al., 2017). Overexpression can be observed in a variety of cancer cells, whereas it is only slightly present in healthy cells (Pubchem). Furthermore, mutations of *XPO1* were found in 0.5-2.9% of solid and haematological tumours, showing the highest frequency in lymphomas (AZIZIAN & LI, 2020).

The inhibitor is currently in clinical trials for AML (NCT02649790). Eltanexor is a second-generation inhibitor of SINE and currently only tested in one clinical trial, recruiting AML patients as well as patients with myeloma, prostate cancer, colorectal cancer and patients with myelodysplastic syndrome (NCT02649790). The advantage of eltanexor compared to selinexor, a first generation SINE inhibitor, and being FDA approved for multiple myeloma in combination with dexamethasone since 2019, is being less toxic in animals; has a lower ability to cross the blood-brain barrier and “does not accumulate in the blood even after repetitive injections” (CAMUS et al., 2017; ETCHIN et al., 2017). For higher-risk myelodysplastic syndrome patients, side effects were minor and eltanexor was well tolerated (LEE et al., 2021; LEE et al., 2022) and for patients harbouring myeloma, side effects were lower compared to selinexor (CORNELL et al., 2022). Due to above listed advantages I decided to use eltanexor instead of selinexor. The published concentration of 15mg/kg oral five times per week was used in the present study (ETCHIN et al., 2017). Human patients received a dose of 10-20 mg/kg five times per week in clinical trials (LEE et al., 2022).

2. Aim of the study

Most current treatment options for ALL are inadequate and an improvement is needed. Here, precision medicine is becoming increasingly important as the basis for the future treatment of tumour patients. Currently mainly descriptive data is used in the clinics e.g. sequencing for mutations or translocations, to assign patients to adjusted therapy. Now we aimed to add a molecular-functional approach to see whether dependencies on a patient individual manner can be uncovered more precisely. The general aim of a larger project was to develop a biomarker to predict treatment response for targeted therapies in individual patients with acute lymphoblastic leukaemia. The molecular screen which functions as a biomarker revealed individual cellular dependencies in PDX ALL cells, this part of the project was conducted by Diana Amend. These dependencies should then predict a response towards a targeting drug. In the future, we aim to convert this concept into a biomarker for clinical applications, using PDX models as surrogates.

The aim of the present subproject was to test the effect of selected targeted therapies against defined PDX ALL models *in vivo* and to correlate the results with existing data from gene dropout. Ultimately, I aimed to understand if hits in molecular dropout screens could predict the response of individual ALL samples towards targeted drugs.

To reduce the usage of mice and improve preclinical drug testing *in vivo*, I further aimed to implement the multiplex *in vivo* assay. Here, individual PDX samples should be tested in parallel in a single mouse, using a competitive *in vivo* approach.

3. Material

3.1. Animal work

The mouse strain NOD.CgPrkdc^{scid} Il2rg^{tm1Wjl}/SzJ (NSG; The Jackson Laboratory, Bar Harbour, ME, USA) is extremely immunodeficient. It lacks in T cells, B cells and natural killer cells. In addition, NSG mice are deficient in multiple cytokine signalling pathways (SHULTZ et al., 2005). Consequently, it enables the engraftment and modelling of the human acute leukaemia (AGLIANO et al., 2008; VICK et al., 2015; EBINGER et al., 2016).

Ethical Statement

Animal experiments were conducted in accordance with the applicable ethical standards of the official committee on animal experimentation (written approval by Regierung von Oberbayern, tierversuche@reg-ob.bayern.de; May 2016, ROB-55.2Vet2532.Vet_02–16-7 and August 2016, ROB-55.2Vet-2532.Vet_03–16-56, ROB-55.2-2532.Vet_02-20-159, ROB-55.2-2532.Vet_03-21-9)

3.2. Animal diet and equipment

Name	Provider
DietGelRecovery	Clear H2O, Westbrook, USA
D12331i Research Diet	Brogaarden ApS, Lynge, Denmark
Conventional pellet diet	Helmholtz Zentrum Munich GmbH, Munich, Germany
Nombrero wet diet feeder	Datesand Limited, Stockport, United Kingdom

Table 1. Animal diet and equipment

3.3. PDX samples

Samples from paediatric or adult acute lymphoblastic leukaemia patients were obtained from the Universitätsspital Zürich Switzerland, Department of Internal Medicine III, Medizinische Klinik campus Innenstadt or the Kinderklinik und Kinderpoliklinik im Dr. von Haunerschen Kinderspital, Ludwig-Maximilians-Universität, Munich, Germany. Samples were collected for diagnostic purposes before start of treatment. Written informed consent was obtained from all patients or parents/caregivers/legal guardians if the patients were minors. The study was performed in accordance with the ethical standards of the responsible committee on human experimentation (written approval by Ethikkommission des Klinikums der Ludwig-Maximilians-Universität Munich, number 068–08 and 222–10) and with the Helsinki Declaration of 1975, as revised in 2000.

No	Sample	Origin
1	ALL-50	Kinderklinik und Kinderpoliklinik im Dr. von Haunerschen Kinderspital, LMU Klinikum, Munich, Germany
2	ALL-199	Kinderklinik und Kinderpoliklinik im Dr. von Haunerschen Kinderspital, LMU Klinikum, Munich, Germany
3	ALL-265	Universitätsspital Zürich, Zürich, Switzerland
4	ALL-502	Kinderklinik und Kinderpoliklinik im Dr. von Haunerschen Kinderspital, LMU Klinikum, Munich, Germany
5	ALL-1034	Klinikum Großhadern, LMU Klinikum, Munich Germany

Table 2. List of PDX samples

3.4.Equipment

Name	Provider
Hettich Rotanta 460 R	Hettich Lab, Tuttlingen, Germany
GM500 Mouse IVC Green Line	Tecniplast, Hohenpeißenberg, Germany
BD FACS Aria III	BD Biosciences GmbH, Heidelberg, Germany
LSR Fortessa x20	BD Biosciences GmbH, Heidelberg, Germany
IVIS Lumina 2	Perkin Elmer, Waltham, USA
Quietek CO2 Induction System	Next Advance Inc., Troy, USA
Gas Anesthesia System XGI-8	Perkin Elmer, Waltham, USA
Gas Filter Canister	Rothacher-Medical GmbH, Heitenried, Schweiz
Incubator Heracell 150i	Thermo Fisher Scientific, Waltham, USA
Microcentrifuge 5425	Eppendorf SE, Hamburg, Germany
Brady BMP	Brady GmbH, Egelsbach, Germany
Microscope primovert	Carl Zeiss Microscopy GmbH, Oberkochen, Germany
Intravenous injection restrainer	Helmholtz Zentrum Munich GmbH, Munich, Germany
Neubauer counting chamber	Optik Labor, Lancing, United Kingdom
Labotect hot plate 062	Labotect Labor-Technik-Göttingen GmbH
Labotect hote plate controller	Labotect Labor-Technik-Göttingen GmbH

Sartorius Quintix precison balance	Sigma-Aldrich, St. Louis, USA

Table 3. Equipment

3.5.Consumables

Name	Provider
TrypanBlue Solution	Sigma-Aldrich, St. Louis, USA
Falcon 15ml, 50ml	Corning Incorporated, Corning, USA
Pipettes 10µl, 20µl, 200µl, 500µl	Starlab GmbH, Hamburg, Germany
Serological pipette 5ml, 10ml, 25ml	Greiner Bio-One GmbH, Frickenhausen, Germany
EasyStrainer 70µM	Greiner Bio-One GmbH, Frickenhausen, Germany
Macs SmartStrainer 70µM	Miltenyi Biotec B.V. & Co. KG, Bergisch Gladbach, Germany
PasteurPipette	??
well plates (6, 12, 96)	Corning Incorporated, Corning, USA
Cellstar CellCulture Flasks T25, T75	Greiner Bio-One GmbH, Frickenhausen, Germany
Microvette 100LH	Sarstedt AG &Co.KG, Nümbrecht, Germany
Needle 24, 26 Gauge	Terumo Agani, Eschborn, Germany
Goldenrod Lancet 5mm	Medipoint, New York, USA
D-Luciferin	Biomol GmbH, Hamburg, Germany
Probe	Helmholtz Zentrum Munich GmbH, Munich, Germany
Cryotube vials	Thermo Fisher Scientific, Waltham, USA
Eppendorf tubes 1,5ml , 2ml	Eppendorf SE, Hamburg, Germany
Accu-jet pro pipette controller	Brand GmbH & Co. KG, Wertheim, Germany
BD Micro-Fine ½ U 0,3ml	Becton Dickinson GmbH, Heidelberg, Germany
Inject-F Luer Solo 1ml	B. Braun Holding GmbH & Co. KG, Meslungen, Germany
Surgical one-time scalpel	B. Braun Holding GmbH & Co. KG, Meslungen, Germany
FACS tubes	Corning Incorporated, Corning, USA

Petri dishes	Greiner Bio-One GmbH, Frickenhausen, Germany

Table 4. Consumables

3.6.Buffers, Media, Solutions

Name	Provider
Phosphate buffered saline	Gibco Life technologies, San Diego, USA
Fetal Bovine Serum	Gibco Life technologies, San Diego, USA
Dimethyl sulfoxide	Sigma-Aldrich, St. Louis, USA
Stem Spam II	Stem Cell Technologies, Vancouver, Canada
Ficoll-Paque Plus	Cytiva Sweden AB, Uppsala, Sweden
DNAse	Roche, Mannheim, Germany
Ethanol	Carl Roth, Karlsruhe, Germany
D-alpha-Tocopherol polyethylene glycol 1000 succinate, BioXtra, water soluble vitamin E conjugate	Sigma-Aldrich, St. Louis, USA
Polyethylene glycol 300	Sigma-Aldrich, St. Louis, USA
Tween80	Sigma-Aldrich, St. Louis, USA
Sodium carboxymethyl cellulose	Sigma-Aldrich, St. Louis, USA

Table 5. Buffers, Media, Solutions

3.7.Chemicals

Name	Provider
Venetoclax (ABT-199)	Selleck Chemicals Llc, Houston, TX, USA
Eltanexor (KPT-8602)	Selleck Chemicals Llc, Houston, TX, USA
S63845	Biozol Diagnostica Vertrieb GmbH, Echig, Germany
Enrofloxacin	Bayer AG, Leverkusen, Germany
Meloxicam	Boehringer Ingelheim GmbH, Ingelheim am Rhein, Germany
Isoflurane	CP-Pharma, Burgdorf, Germany
L-Glutamin	Gibco, San Diego, USA
Penicillin/Streptavidin	Gibco, San Diego, USA

Table 6. Chemicals

3.8.Antibodies

Name	Provider
Anti-H-2Kk	Miltenyi Biotec B.V. & Co. KG, Bergisch Gladbach, Germany
CD45 APC	Becton Dickinson GmbH, Heidelberg, Germany
PE mouse Anti-human CD33	Becton Dickinson GmbH, Heidelberg, Germany
APC anti-human CD19	BioLegend
Hu CD271 BV711 C40-1457 50µg	Becton Dickinson GmbH, Heidelberg, Germany

Table 7. Antibodies

3.9.Constructs

Name	Generated by
pCDH-EF1-H2Kk+BC5	Diana Amend
pCDH-EF1a-iRFP720+BC7	Diana Amend
pCDH-EF1-enFFly-T2A-mCherry	Addgene: Addgene ID: 104833
pCDH-EF1-enFFly-T2A-mtagBFP+BC3	Diana Amend
pCDH-EF1-enFFly-T2A-NGFR+BC1	Diana Amend
pCDH-EF1-eFFly-T2A-T-Sapphire+BC9	Diana Amend
pCDH-SFFV-YN-N-Cas9-N-Intein + pCDH-SFFV-Cintein-C-Cas9-P2A-CC	Martin Becker

Table 8. Constructs

3.10. Flow cytometry settings

LSRFortessa X20:

Laser (nm)	Longpass Filter (nm)	Bandpass Filter (nm)	Parameter
375/405	502	450/40	mTagBFP
405	505	525/50	T-sapphire

405	690	710/50	BV7-11
488	502	530/30	eGFP
561	600	610/20	mCherry, PE Texas red
640	690	730/45	iRFP
640	690	670/30	APC

Table 9. LSRFortessa X20 settings

FACS Aria III:

Laser (nm)	Longpass Filter (nm)	Bandpass Filter (nm)	Parameter
405	505	450/40	CFP
405	502	530/30	T-sapphire
405	685	710/50	BV-711
488	502	530/30	eGFP
561	600	610/20	mCherry
633	750	780/60	APC-cy7

Table 10. FACS Aria III settings

3.11. Software

Name	Provider
Living Imaging Software	Caliper Life Sciences, Waltham, USA
MyIMouse	BIOSLAVA GbR, Berg, Germany
Graphpad Prism 9	GraphPad Software, San Diego, USA
FlowJo v.10.6	BD FlowJo, Ashland, USA
RStudio	RStudio, Boston, USA
MS Office	Microsoft Corporation, Redmond, USA
Biorender	Biorender, Toronto, Canada

Table 11. Software

4. Methods

4.1.Mice

4.1.1. Housing

NSG mice were housed under specific pathogen-free (SPF) conditions in individually ventilated cages. Light cycle includes 12/12 hours. According to Annex A of the European Convention 2007/526 EC the temperature was 20-24°C and humidity ranges from 45 to 65%. A maximum of five mice were kept per cage in line with the policy Annex III of the 2010/63 EU. Mice had access to structural enrichment and unlimited food and water.

4.1.2. End points

The animals were inspected daily and scored weekly. When medium stress was reached, the animals were scored daily. Monitoring characteristics included body condition score (BCS), posture and movement, behaviour, grooming condition, eyes and respiration (see appendix). Human endpoints were a BCS of <1, marked lameness or inability to move. Animals with apathetic behaviour and no response to external stimuli, as well as swollen eyes or abdomen and panting, also led to termination. In treatment trials, a loss of body weight of more than 15 % over more than two days or of more than 20 % compared to the day of treatment initiation led to discontinuation. Mice that died under inhalation anaesthesia were excluded from further analyses. Mice that had disease unrelated to leukaemia were excluded from the studies, as were mice that did not show engraftment of human cells.

4.2.The Patient Derived Xenograft Mouse Model

Primary patient samples of ALL were transplanted into NSG mice to generate the PDX model for acute leukaemia.

4.2.1. Engraftment and Expansion

4.2.1.1. Thawing samples

Frozen primary or PDX samples were thawed in 37°C water for 3 minutes. Then 1mg/ml DNAse, consisting of 6µl pure DNASe and 94µl PBS (phosphate buffered saline), are added. After mixing 1 ml FCS is added. Followed by 10ml PBS/2% FCS and one minute of incubation. Additionally, 30ml PBS/2% FCS is used and mixed and another minute is needed. The sample is centrifuged at 200g RT for five minutes. Supernatant is dissolved and 10ml fresh PBS added and cells are counted (see 4.5.1.2).

4.2.1.2. Counting of cells using Neubauer counting chamber

50µl sample is added to 400µl PBS and 50µl Trypanblue. Out of this mix 10µl are transferred to the Neubauer counting chamber and cells were counted.

Each result out of one of four squares is added and divided with four to get the mean value. This number x multiplied with 10 = y. This number y divided with 100 to receive the number of cells in 1 ml.

4.2.1.3. Injection of cells

Up to $1x10^7$ fresh or cryopreserved primary human leukaemia cells, pre-leukemic cells or PDX cells are suspended in 100-150µl PBS and transplanted into the tail vein of non-irradiated 6-24 weeks old male or female NSG mice.

4.2.1.4. Sacrifice with CO2 exposure

Mice were sacrificed by carbon dioxide using the Quietek CO2 Induction Systems initially wat a flow rate of 20% of the chamber volume per minute for 5 minutes to anesthetized the animals. Followed by 100% of the chamber volume per minute for additional 3 minutes to kill the mice. Death of the animals was determined before removal of organs or cervical spine.

4.2.1.5. Sacrifice with cervical dislocation

Mice were picked up and placed on the wire of the cage or flat surface. The thumb is placed on the neck. The cervical dislocation is performed by a rapid forward and downward thrust of the thumb while the tail is pulled backwards to stretch the body. Death was determined by palpating the region between occipital condyles and first cervical vertebra. Additionally, respiratory and heart rates were checked.

4.2.1.6. Isolation of PDX cells from the bone marrow

After sacrificing the mouse; tibia, femur, coxis, sternum and chorda spinae were extracted. Bones are crushed in a mortar and moisturize with 1-2ml PBS. The cells are transferred through a cell strainer into a 50ml Falcon that contains 10ml PBS. The suspension is centrifuged 5min, 400g at room temperature. The cell pellet was re-suspended in 10 ml PBS and used for further analysis.

4.2.1.7. Isolation of PDX cells from the spleen

After sacrificing the mouse, the spleen was extracted. The spleen was squashed through a cell strainer into a petri dish. The cell suspension is transferred through a cell strainer into a 15ml Falcon and filled up with 10ml PBS. The cell suspension was underlaid with a long needle including 10ml Ficoll. Cells were centrifuged 30min, 400g at 22°C. After centrifugation an interphase consisting out of mono-nuclear cells appeared. This interphase was aspirated with a Pasteur pipette and transferred into a 15ml Falcon. Cells were washed with 10ml Falcon and centrifuged 10min at 400g, 22°C. Afterwards the cells were re-suspended in 10ml PBS and counted by using the Neubauer counting chamber.

4.2.1.8. Passaging of PDX cells

Patients' leukaemia cells are transplanted into immunodeficient mice to generate the PDX model, as mentioned earlier. The leukemic cells were re-isolated from the bone marrow and spleen and re-injected into the next recipient mice for several passages to enable repetitive in vivo analyses. Furthermore, PDX cells are genetically engineered by lentiviral transduction.

4.2.1.9. Genetically engineered PDX cells

PDX cells were genetically engineered by lentiviral transduction. The cells were marked with constructs expressing Cas9 and sgRNA libraries to enable CRISPR/Cas9 dropout screens. Enhanced firefly luciferase to monitor the leukaemia growth by using bioluminescence *in vivo* imaging. Fluorochromes and tags enabled distinction of the samples by their individual colour.

PDX cells were isolated from mouse spleen or bone marrow and resuspend in medium. $10x10^6$Cells were cultured in 1 ml and transferred into a 12-well plate. 4µl of the virus, including the construct, were added in the presence of 4µl polybrene. After 24 hours, cells were re-suspended and centrifuged 5min, 400g at room temperature. Cells were washed 3 times with 14ml PBS, centrifuged at 300g, 5min

at RT. Afterwards re-suspended in 10 ml Stempspan II media and transferred into a T75 flask. After 5 days aimed transduction efficiency of 30% was reached and injected into mice.

Five PDX samples have been lentivirally transduced with different recombinant fluorochromes (see 3.10) by Diana Amend, who designed and cloned the constructs for all five samples.

4.2.2. Sorting

After re-isolating cells from transduced samples, cells were sorted using the BD FACS Aria III. Up to $1x10^6$ Cells were suspended in 0,5ml PBS and sorted via fluorescent activated cell sorting. PDX samples were gated for living cells in the forward sideward scatter and then for the expressed fluorochrome.

4.2.3. Flow cytometric analysis

Flow cytometry describes the measurement of cells in a fluid stream detected by a light beam, determining physical properties of cells such as size, granularity or internal complexity and fluorescence intensity. The light signals are converted into an electronic signal that enables evaluation on a computer. (ADAN et al., 2017)

Cells were analysed via flow cytometry using a BD LSRFortessa X20 or BD FACS Aria III. For the detection of the expressed fluorochromes (eGFP, iRFP, mCherry, mtagBFP, T-sapphire) and other fluorophores (APC, PE, BV7-11) the following laser settings were used (see 3.10). For the detection of H2K-k and tNGFR marked cells, cells were stained, as described below.

4.2.3.1. Staining for flow cytometric analysis

Cells marked with tags can be detected in flow cytometry due to a fluorescent dye which is conjugated to an antibody (VALTIERI et al., 1994). For the detection of H2K-k marked cells, 1 million cells were stained with 1 µl H2K-k Antibody, anti-mouse, APC. For NGFR marked cells, 1 million cells were stained with 5µl of Hu CD271 BV711 C40-1457 50µg. The cells were kept in the dark for at least 20 minutes. After incubation, 1ml PBS was added in order to wash the cells and remove the antibody. After 5 minutes centrifugation (400g RT) 100-200µl PBS were added and stained cells were measured in flow cytometry.

4.2.4. Monitoring of engraftment

4.2.4.1. Blood sampling for blood measurement

Intravenous (i.v.):

Mice were fixed in a restrainer and the tail vein was disinfected with 80% Ethanol. The needle (Gauge 24-26) pierced the vessel and the blood (approx. 50µl) was collected in a Microvette 100 LH. Pressure was then applied to the puncture wound.

Vena facialis:

The animal was fixed in the neck grip and the cheek is tightened. A blood lancet was used to briefly puncture and release the tension. Up to 50 µl of the outflowing blood was collected with a Microvette 100 LH.

4.2.4.2. Flow cytometric analysis for blood measurement

To monitor the engraftment of human cells, 50µl blood was obtained from the tail vein. The sample was stained with 5µl CD45mu-APC and 5µl CD38hu-PE and incubated 30min at room temperature. After washing with 3ml FACS buffer and centrifuged at room temperature, 300g, the cells were measured via flow cytometry using BD LSRFortessa X20. Positivity for CD38 was used to detect ALL.

4.2.4.3. Bioluminescence – monitoring engraftment of PDX cells

The IVIS Lumina 2 was used to measure Bioluminescence and to monitor the engraftment of the leukemic cells in mice. Mice were anaesthetized with isoflurane in an inhalation chamber. For cells expressing a firefly luciferase, 150 mg/kg D-Luciferin was injected into the tail vein. The picture recording time ranged from 30 seconds to two minutes. A field of view of 12.5 cm with binning 8, f/stop 1 and open filter setting was used as a standard setting. Pictures with more than 1000 counts were considered within the linear range and saturated pictures were repeated with reduced exposure time or reduced f-stop.

4.2.4.4. Anaesthesia

For *in vivo* imaging, animals were sedated with inhaled isoflurane. Initially, animals were placed in the anaesthesia chamber, flooded with 1.2 L/min of a mixture of oxygen with 5% isoflurane. After failure of the stellate reflex, the isoflurane concentration was reduced to 1.5%. The animals were placed on their backs in the imaging device and received anaesthesia via a tube with a funnel at the end, which was held directly in front of the nose of the anaesthetised animals.

4.2.4.5. Quantification of BLI pictures

The analysis of the bioluminescence pictures was conducted using the Living Image software. The region of interest (ROI) which is covering the whole mouse was use and total flux was determined.

4.2.5. Competitive transplantation assay

For the competitive transplantation assay five ALL samples (ALL-50, ALL-199, ALL-265, ALL-502 ALL-1034) were thaw and mixed. Five PDX samples, “were multiplexed and aliquots injected into groups of mice (n=3-6). For post mortem analysis, PDX cells were re-isolated from murine bone marrow and absolute tumour burden of PDX cells was quantified by flow cytometry of exactly 1/10 of the bone marrow. Determining fluorochrome composition allowed quantifying the proportion, that each of the five samples contributed to the entire tumour load. In case of treatment, a response rate for each individual sample was determined by comparing cell numbers in treated versus control mice.” (HUNT et al., 2022)

4.2.5.1. *In vivo* therapy trial

One of the following drugs, see below, was dissolved and administrated via oral gavage or intra venous at the depicted concentration for the depicted time phrase. To depict the exact concentration the body weight was monitored before and during the therapy trial. Therapy started when total flux reached a certain value (total flux = $1x10^9$ photons/seconds).

Three experimental groups were set:

1. Therapy start – these mice were sacrificed before the therapy started to determine the proportion of each sample to the entire tumour load in the beginning of the trial.
2. Mice who received therapy and

3. The control group, which received solvent.

The groups consist out of five to six animals each.

Drug	Concentration	Route of application	Amount	Duration	Function
Venetoclax (ABT-199)	100mg/kg	p.o.	5x/week	2 Weeks	BCL2 Inhibitor
Eltanexor (KPT-8602)	15mg/kg	p.o.	5x/week	2 Weeks	XPO1 Inhibitor
S63845	25mg/kg	i.v.	2x/week	2 Weeks	MCL1 Inhibitor

Table 12. Treatment scheme of compounds used for multiplex *in vivo* preclinical trials

4.2.6. Application and fixation methods

Per os

At first, the correct cannula size was determined. The cannula should not be longer than the distance from mouth to the middle of the stomach. The mouse was fixed in the neck scruff and was slightly overstretched backwards due to the usage of rigid cannulas. Application is advance into the stomach via the base of the tongue.

i.v.

A restrainer was used for fixation and the sample/substance is injected into the tail vein.

s.c.

The mice are hold in the scruff neck fixation. The neck fur is hold with thumb and index to inject into the resulting skin fold.

4.3. Statistical analysis

Statistical analysis was performed using GraphPad Prism 7 software. For *in vivo* studies the two-tailed t-test with Welch Correction was applied. (*$p < 0.05$, **$p < 0.01$, ***$p < 0.001$, ****$p < 0.0001$).

5. Results

The general aim of a larger project was to develop a biomarker to predict treatment response for targeted therapies in individual patients with acute lymphoblastic leukaemia. According to the concept of targeted therapies, loss of a given target gene should predict treatment response to a drug targeting that same gene. We aimed to convert this concept into a biomarker for clinical use, using PDX models as surrogates. Here, CRISPR/Cas9 screens were performed with a customized library in PDX samples. The aim of the present subproject was to test the effect of selected targeted therapies against defined PDX ALL models *in vivo* and to correlate the results to existing data from gene dropout.

5.1.Selection of drugs and compounds

5.1.1. CRISPR/Cas9 screen in PDX reveal dependencies on a patient-individual manner

Diana Amend transduced the stable Cas9 expressing PDX samples with the sgRNA library including the 146 targets with 5 sgRNAs per target with a low transduction efficiency of maximum 30%. Low transduction efficiency aims to result in single genomic integration. After enrichment of transgenic cells *ex vivo*, cells were injected into groups of mice. When overt leukaemia developed, mice were sacrificed, cells were re-isolated from bone marrow and spleen, and gDNA was isolated. Afterwards, DNA was sequenced using next-generation sequencing to determine the sgRNA frequency and analysed using MAGecK (Model-based Analysis of Genome-wide CRISPR-Cas9 Knockout) as described in Wirth et al (2022). Hereby, the following dependencies were detected:

ALL-50	ALL-199	ALL-265	ALL-502	ALL-1034
BCL2	*BCL2*	*BCL2*	*BCL2*	
MCL1	*MCL1*		*MCL1*	
XPO1	*XPO1*	*XPO1*	*XPO1*	*XPO1*

Table 13. CRISPR/Cas9 dropouts in five PDX samples

Now it was my task to investigate these dependencies in preclinical treatment trials using targeted drugs to determine if these drugs are effective in individual PDX samples in a way which correlated to the molecular data.

5.1.2. Criteria's for drugs to use in preclinical *in vivo* trials

To correlate and individual dropout with response towards a targeting drug, a drug was selected while considering the following criteria:

a. A specific and direct drug has to be available, implicating that the drug targets the gene directly and highly specific. A drug was excluded if it inhibits cross-connected pathways or if other targets in a pathway were co-targeted. For example, navitoclax targets *BCL2* but also *BCL-XL* and *BCL-WL*, whereas venetoclax only inhibits *BCL2* (ROBERTS et al., 2021), so venetoclax was selected.
b. Literature of *in vivo* usage of the drug in mice was required, since we are not allowed to test substances without prior knowledge of toxicity and effectivity.

As a result, venetoclax, S63845 and eltanexor, were selected for preclinical *in vivo* trials to correlate results with existing data from gene dropout *BCL2, MCL1* and *XPO1*.

5.2. Establishing PDX models for the usage of multiplex *in vivo* assays

In order to define prediction accuracy of molecular dropout screens as a biomarker to identify personalized targets for pharmacological approaches, the aim of the present study was to correlate existing data from CRISPR/Cas9 dropouts with preclinical *in vivo* treatment trials. Here, the molecular hits shall be correlated with a corresponding response towards a targeting drug. Additionally, the aim was to increase the efficiency of preclinical trials *in vivo* by simultaneously testing multiple individual samples in parallel in a single mouse (HUNT et al., 2022). As mentioned in 1.3.4 this *in vivo* assay is termed as "multiplex *in vivo* assay" in the present study.

5.2.1. Selection of suitable PDX models

In the hosting laboratory, 226 ALL patient samples had been transplanted into NSG mice, of which 138 engrafted. 70 ALL allowed serial transplantation and thus are repetitively available for *ex vivo* and *in vivo* experiments.
To enable multiplexing, the samples had to meet the following criteria:

1. show a reliable engraftment of leukemic cells, to evaluate the response of drugs in a competitive approach and
2. Show a similar passaging time, which indicates the time needed for each sample to develop overt leukaemia. In order to mix the cells, a similar passaging time was needed to ensure no suppression of slower samples within a mouse takes place.
3. are transgenic for enhanced firefly luciferase to allow repetitive monitoring of leukaemia growth and treatment response using bioluminescence *in vivo* imaging (BLI)

No	Sample	Age (Years)	Sex	Disease stage	Leading genetic abnormality
1	ALL-50	7	f	diagnostic	t(1;19) TCF3::PBX1
2	ALL-199	7	f	relapse	germline +21; somatic homozygous 9p deletion (CDKN2A); P2RY8::CRLF2
3	ALL-265	5	f	relapse	High hyperdiploidy
4	ALL-502	9	f	relapse	IGH::DUX4
5	ALL-1034	20	m	relapse	ETV6::ABL1 (Ph-like)

Table 14. Characteristics of ALL PDX samples

5.2.2. Engraftment and passaging time of PDX samples

To gain insights into the *in vivo* engraftment capacity of the PDX samples in the hosting laboratory, the internal mouse database was studied and data from 2014 until 2022 were analysed.
First, engraftment capacity (mice with positive engraftment related to all transplanted mice) was determined, which ranges from 95.8% to 99.4% for the selected ALL samples. The best engraftment rate can be seen for ALL-50 with 99.4% and the least good ALL-265 95.8% (figure 2A).

Second, passaging time of each PDX sample was determined from mice injected between 2019 and 2022. Here, only mice were included which were transplanted with Cas9 transgenic cells. Average passaging time of the selected samples ranged from 35 to 51 days.

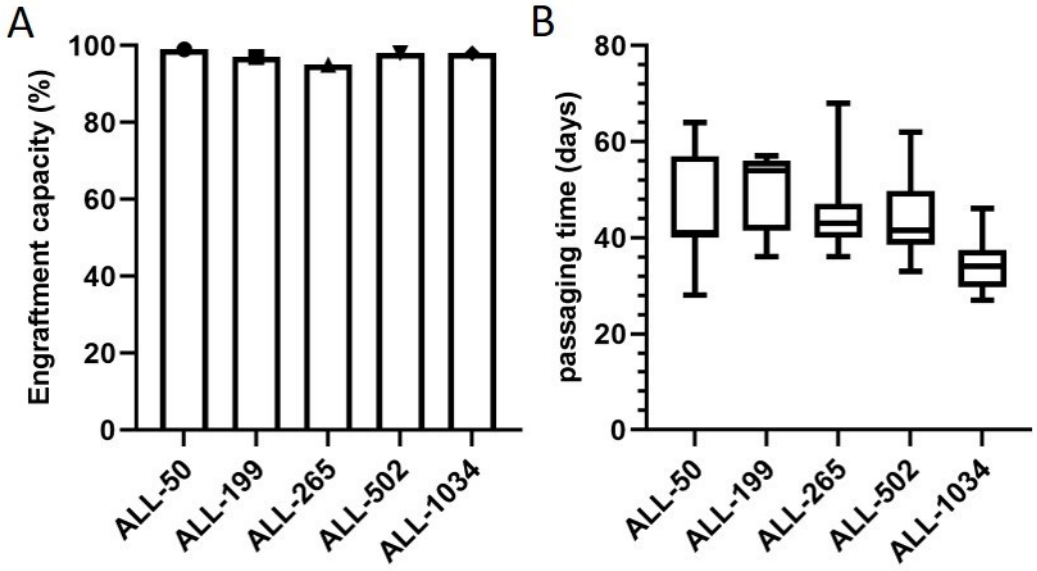

Figure 2. Engraftment characteristics of PDX samples

a. Bar plots depicting percentage of transplanted mice with positive engraftment for each PDX sample. Positive engraftment indicates leukemic cells could be re-isolated after sacrificing mice. Mice were injected with a variety of cell numbers and analysed at different time points. ALL-50: n=169; ALL-199: n=638; ALL-265: n=571; ALL-502: n=81; ALL-1034: n=59.
b. Box plots depicting passaging time. Mice were injected with $1x10^4$ to $1x10^7$ split-cas9 transgenic PDX cells, and sacrificed at overt leukaemia. ALL-50: n=12; ALL-199: n=14; ALL-265: n=12; ALL-502: n=10; ALL-1034: n=10.

As a result, five ALL samples were included into the project. They show a reliable engraftment of leukemic cells, a similar passaging time and are transgenic for enhanced firefly luciferase. The selection of the samples includes all age classes for ALL and represents a variety of different genotypes. Material from patients with relapses predominate; one diagnostic sample is also present.

5.3. Genetic labelling of individual ALL PDX samples with unique fluorochromes to allow multiplex *in vivo* assays

Diana Amend transduced the five selected ALL samples with unique lentiviral constructs containing a fluorochrome (iRFP720, mTagBFP2, T-Sapphire) or molecular tag (tNGFR or H2-Kk) to allow tracking each sample *in vivo* over time by flow cytometric based readout in multiplexing trials (WIRTH et al., 2022). Fluorochrome and tag marked cells were enriched using flow cytometry activating cell sorting and transplanted into the next recipient mice. This step was repeated until at least 90% of the cells expressed of the fluorochrome or tag, after re-isolation from bone marrow and spleen. Transgenic samples were expanded and viable frozen for upcoming multiplex *in vivo* trials.

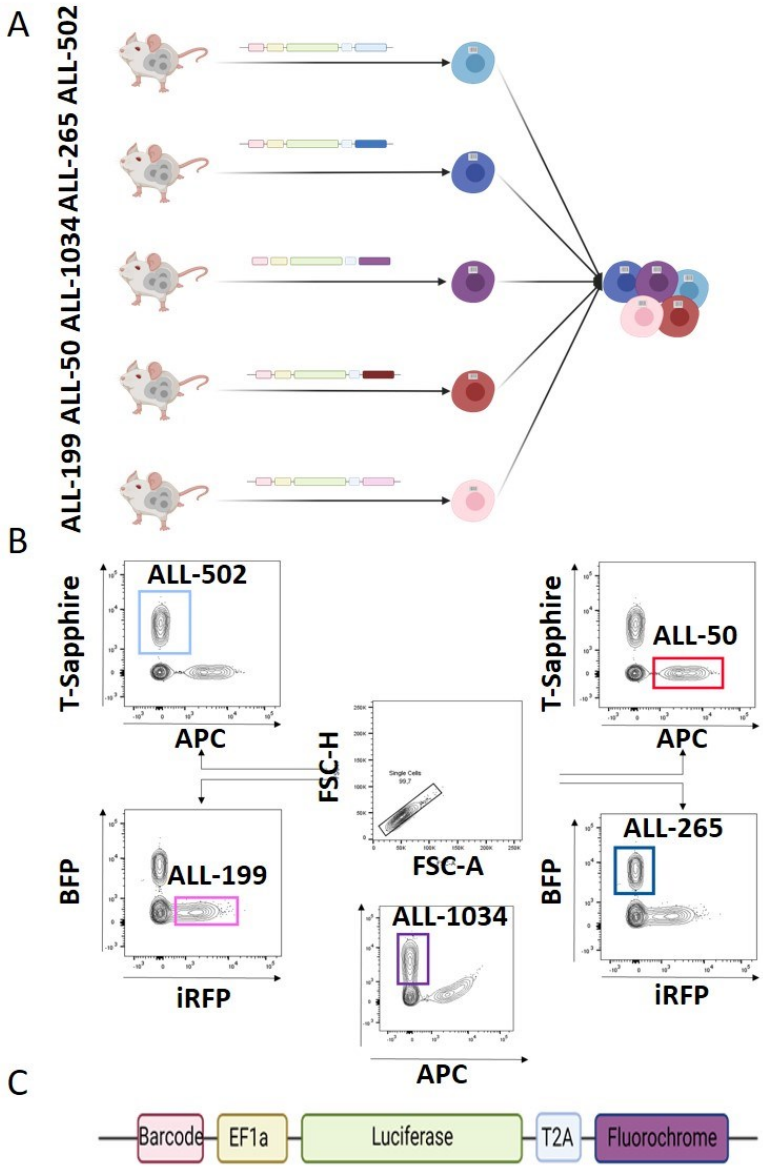

Figure 3. Labelling individual PDX samples with unique fluorochromes

A. Five PDX samples were transduced with a unique fluorochrome. B. Exemplary gating strategy in flow cytometry. Gating for single cells and afterwards for the unique fluorochromes. Determining fluorochrome allows quantifying absolute numbers of individual samples composition. C. Exemplary construct - the construct consists of a barcode, EF1a promoter, luciferase, T2A self-cleaving peptide and individual fluorochrome or tag.

5.3.1. A defined mixture is needed to enable multiplex *in vivo* assays

This study aimed to increase the efficiency of preclinical trials *in vivo* by simultaneously testing multiple individual samples in parallel in a single mouse, using the multiplex *in vivo* assay. (HUNT et al., 2022) Since the samples showed a similar passaging time (see 5.2.2), I decided to inject the fluorochrome labelled samples in a homogeneous mixture. PDX cells from donor mice were thawed, mixed in a 1:1 ratio, and transplanted into two groups of mice. Tumour outgrowth was monitored by *in vivo* bioluminescence imaging (BLI). Two different time points after transplantation, mice were sacrificed. PDX cells were re-isolated from bone marrow and amount each PDX sample was analysed by flow

cytometry. Flow cytometry data revealed that all samples engrafted homogeneously, despite ALL-502, which was overrepresented at both time points (figure 4A; 4B).
Importantly, an increase of tumour burden between the two time points could only be seen in the samples ALL-50 and ALL-502, while ALL-265 and ALL-1034 remained stable, and ALL-199 even showed a reduction of tumour load (figure 4B). As this effect of a stop in tumour growth or even reduction of tumour load has never been observed in non-competitive trials with these data before (data not shown), we hypothesised that the overpopulation of ALL-502 might inhibit the other samples. Therefore, we concluded that an adjusted mixture might be necessary to circumvent this effect.
Taken together, competitive transplantation of five PDX samples is possible. However, an adjustment of the injection mix is needed, to ensure a homogeneous distribution of all five samples in order to be able to analyse samples equally well.

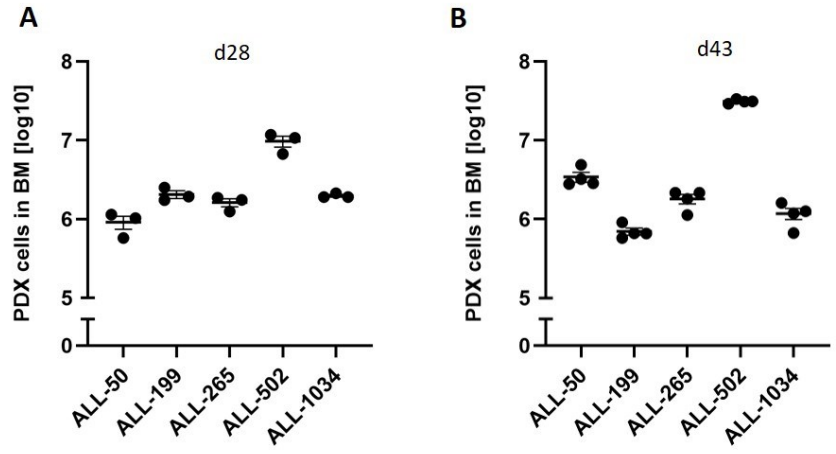

Figure 4. Competitive transplantation of five ALL PDX samples at a homogeneous ratio
Amount of individual ALL PDX cells isolated from bone marrow (BM) of mice sacrificed 28 days (A, n=3) or 43 days (B, n=4) after transplantation. Each dot represents one mouse. Mean SEM+- is shown.

5.3.2. Adjusted mixture ensures homogenous engraftment for multiplex *in vivo* assays

Due to the fact, that ALL-502 showed an increased growth (see 5.3.1), an adjustment of the injection mixture was necessary; a disadvantage of a factor ten was chosen for ALL-502. Again, samples were thawed, counted, mixed and injected into groups of mice. Engraftment of cells was monitored using bioluminescence *in vivo* imaging. After different time points, mice were sacrificed. PDX cells were re-isolated from bone marrow and spleen, and ratio of the PDX samples was analysed by flow cytometry. As expected, with increasing bioluminescence values, the number of leukemic cells increased both in bone marrow (figure 5A;5B) and in spleen (figure 5C).
In spleen, however, leukemic cells were detectable only from day 21 on, while they were above flow cytometric detection limit in bone marrow at all analysed time points.
The amount of PDX cells isolated from individual mice was homogeneous within a sample at each time point; however, the samples are heterogeneous in mice between samples at all-time points. It is not always the same sample with higher abundance. Differences are acceptable for this approach, as all samples can be analysed at each time point, and abundance of all samples increases over time.
In summary, this mixture is suitable for further preclinical trials and ensures a homogeneous distribution of all five samples in order to be able to analyse samples equally well.

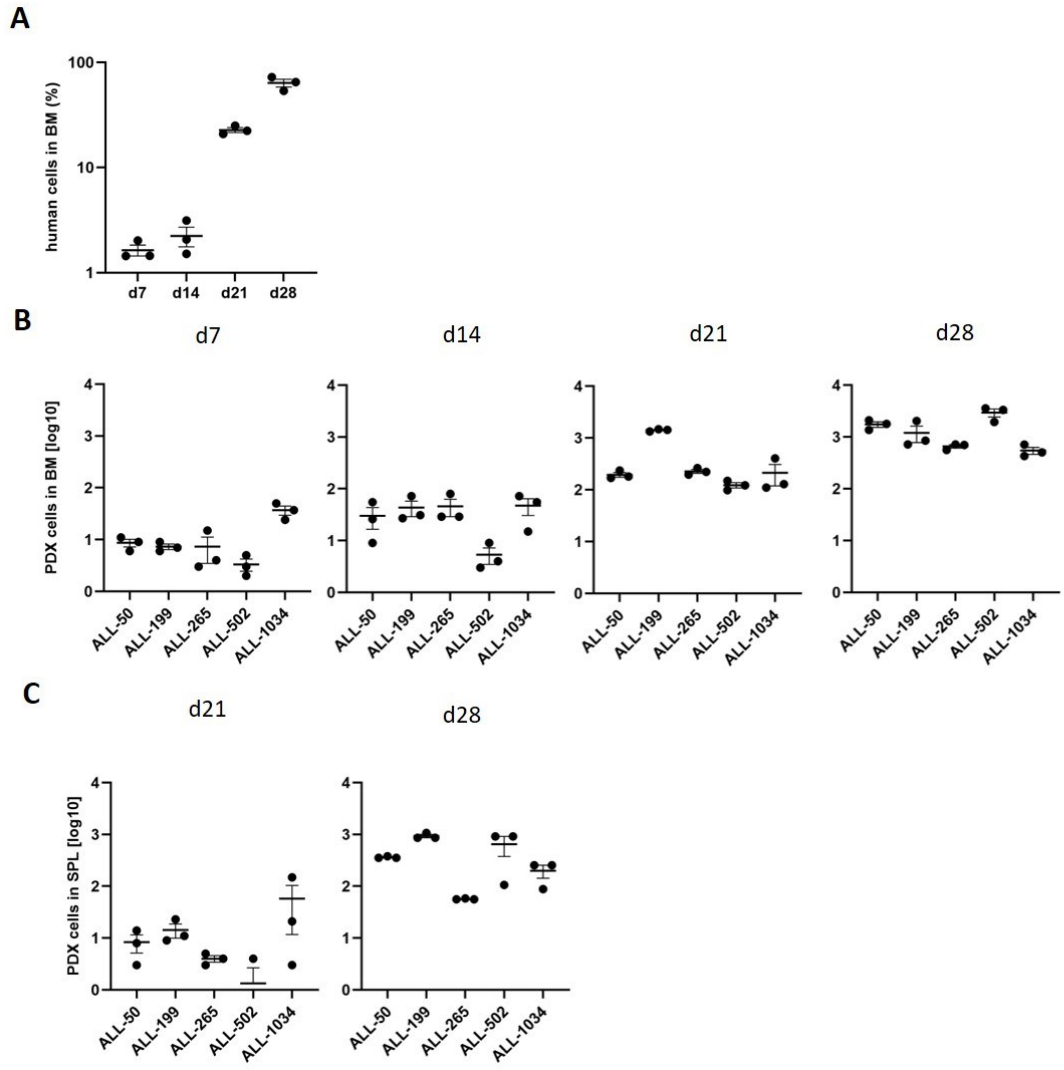

Figure 5. Competitive transplantation of five ALL PDX samples with an adjusted mixing ratio

a. Percentage of ALL PDX cells (combined analysis of all samples) in bone marrow (BM) for all four time points. Each dot represents one mouse (n=3). b. Absolute cell number of individual PDX cells in bone marrow BM 7, 14, 21 and 28 days after injection. Each dot represents one mouse. c. Absolute cell number of individual PDX cells in spleen (SPL) 21 and 28 days after injection. Each dot represents one mouse.

5.3.3. Reproducibility of the multiplex *in vivo* assay

This approach was then used in preclinical multiplex *in vivo* assays to test the efficacy of selected targeted therapies (see 5.4). To understand if this new established approach showed reproducible results not only within a trial but also in independent experiments, I compared engraftment of the five samples at two time points in the three independent therapy trials explained below.

As depicted in figure 6, competitive transplantation resulted in a homogeneous engraftment of each individual PDX sample in all three independent multiplex *in vivo* assays conducted in the present study (see 5.4). Especially the engraftment of ALL-199, ALL-502 and ALL-1034 was consistent and highly reproducible. Growth of ALL-50 and ALL-265 showed some variances between but not within the trials. These data indicate a stable system and strong reproducibility between experiments.

With this approach, I established a novel competitive preclinical testing approach for ALL PDX *in vivo*. With this approach, the effect of a single drug can be determined in parallel in up to five different samples, allowing the reduction of resources by factor 5, in line with the 3 R concept.

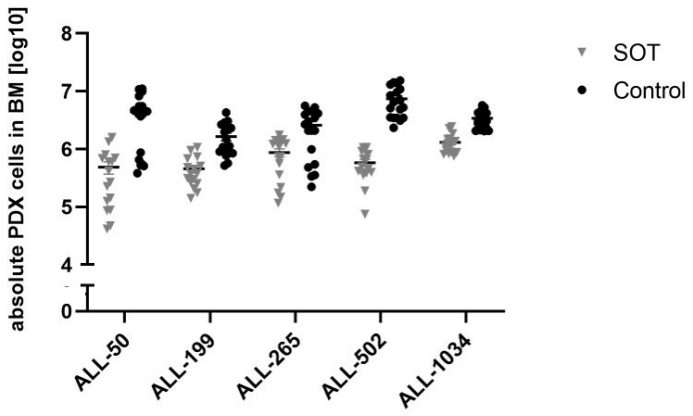

Figure 6. Summary of three independent multiplex *in vivo* trials

Grey: mice sacrificed at the time point start of therapy (SOT) (n=18). Black: untreated mice (Control), sacrificed at the time point end of therapy (n=18). Each dot represents one mouse (mean±SEM). Figure combines data presented in figures 8, 11 and 12.

5.4. Preclinical multiplex *in vivo* assay to test the efficacy of selected targeted therapies

Preclinical treatment trials were conducted using the multiplex *in vivo* assay. Selected targeted therapies were administrated to determine response of individual samples, and to determine if results of pharmacological testing correlate with dropout results of molecular targeting.

5.4.1. Targeting *BCL2* with venetoclax revealed response in two out of five ALL samples

The molecular *in vivo* screens revealed a dropout of *BCL2* in four ALL samples (ALL-50, ALL-199, ALL-265, ALL-502), suggesting a putative response in these samples towards an inhibition of this anti-apoptotic protein, while one sample without a dropout in *BCL2* might be resistant (ALL-1034).
To determine if samples, which show a dropout of *BCL2,* are also sensitive towards a pharmacological inhibition of BCL2 *in vivo*, mice were treated with the specific BCL2 inhibitor venetoclax (ABT-199). PDX cells from donor mice were thawed, mixed as in 5.3.2, and transplanted into three groups of mice. Tumour outgrowth was monitored by *in vivo* bioluminescence imaging (BLI).

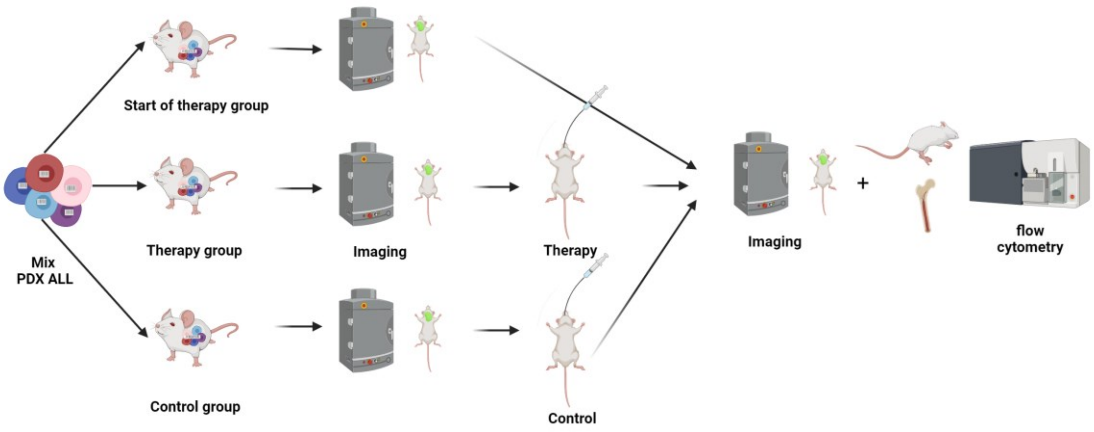

Figure 7. Experimental set up for multiplex *in vivo* preclinical treatment trials

Mixed cells from five different ALL PDX samples labelled with a unique fluorochrome (see figure 3) were injected into three groups of NSG mice ("start of therapy", "therapy" and "control" group, n=6 per group). Tumour burden was monitored by BLI. After successful engraftment, mice from start of therapy group were sacrificed, bone marrow was isolated, and absolute cell number of PDX cells before treatment start was measured by flow cytometry. Remaining mice were treated repetitively with either a specific drug or with solvent as control for two weeks. 4 to 5 days after stop of treatment, mice were sacrificed. For post mortem analysis, PDX cells were re-isolated from murine bone marrow and absolute cell number of PDX cells was quantified by flow cytometry of exactly 1/10 of the bone marrow. Determining fluorochrome composition allowed quantifying the number of cells, that each of the five samples contributed to the entire tumour load. In case of treatment, a response rate for each individual sample was determined by comparing cell numbers in treated versus control mice.

All mice showed physiological behaviour and a good body condition. When leukaemia developed a defined leukaemia burden in BLI (total flux = $1x10^9$ photons/seconds), the mice of time point start of therapy were sacrificed and analysed. Flow cytometry data revealed that all samples engrafted homogeneously (figure 8F).

The other groups of mice were treated for 2 weeks with either venetoclax or solvent as control. Four to five days after the last dose, mice were sacrificed and bone marrow and spleen were analysed. Mice were in a good condition and showed physiological behaviour.

The BLI signal was reduced in venetoclax treated mice compared to control mice at the end of therapy (figure 8A;8B). The total amount of human cells present in the bone marrow, i.e. the amount of five PDX samples, was also decreased in treated compared to control mice (figure 8C). These data indicate, that the mix of ALL PDX cells was reduced by the therapy in the treated mice. No significant reduction in spleen weight was observed after treatment (figure 8D). Body weight was minimally reduced in treated mice and constant in all mice (figure 8E), indicating that venetoclax therapy was well tolerated.

Notably, the absolute numbers of ALL-50 and ALL-265 in bone marrow showed a drastic decrease in venetoclax treated mice compared to control, while ALL-199, ALL-502 and ALL-1034 showed no reduction of leukemic cells in venetoclax treated mice. This effect could be detected in flow cytometry, in cells isolated from bone marrow. Variances between mice were in general minor, with few exceptions in some treated mice (figure 8F).

Strikingly, we can observe a leukemic cell reduction in ALL-50 and ALL-265, if we compare start of therapy cells with the treated cells.

Taken together, a reduction of leukemic cells can be observed for ALL-50 and ALL-265, but not for ALL-199, ALL-502 and ALL-1034. These data indicate that venetoclax might cause cell death in ALL-50 and ALL-265 and does not affect ALL-199, ALL-502 and ALL-1034 cells.

In summary, the aim was to determine if samples, which show a dropout of *BCL2,* are also sensitive towards a pharmacological inhibition of BCL2 *in vivo*, which is true for two of five PDX samples.

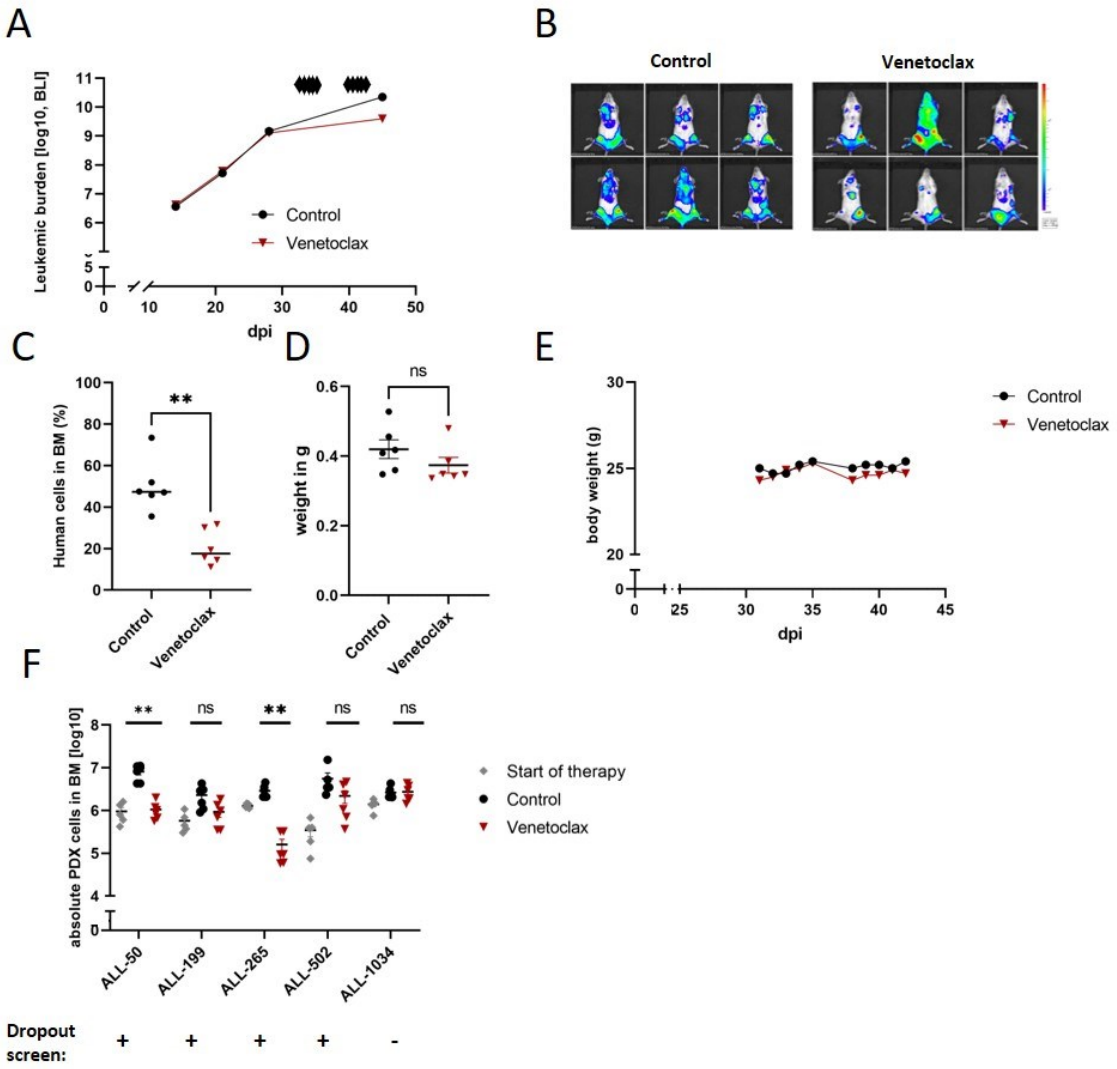

Figure 8. Targeting BCL2 with Venetoclax with a novel multiplex *in vivo* assay

Experiment was performed as described in figure 7. 21 days after injection, mice were treated with ten doses of venetoclax (100 mg/kg; n=6) or solvent as control (n=6) per os. Mice were sacrificed on day 44/45 after injection.

a.Quantification of bioluminescence *in vivo* imaging signals of control (black) and venetoclax treated mice (red), diamonds indicate days of therapy. b. individual pictures on day 43 after injection. c. Percentage of human cells present in bone marrow (BM) in control and treated mice on day 44/45 after injection (mean ± SEM, p=0.0011 by Welch t-test). d. Spleen weight of control and treated mice on day 44/45 after injection (mean ± SEM, p=0.2182 by Welch t-test). e. Body weight of mice during therapy (mean). f. Analyses depicting each PDX population. Absolute cell numbers for each sample is indicated for BM. Comparison of mice time point start of therapy (grey) with control (black) and treated mice (red). Each dot represents one mouse. Mean ± SEM is shown. Statistical analysis was performed by Welch t-test: ALL-50: p=0.0022, ALL-199: p=0.0571, ALL-265: p=0.0010, ALL-502: p=0.1499, ALL-1034: p=0.8693

5.4.2. Preclinical treatment trial of a single PDX shows consistent results with the multiplex *in vivo* assay

To quality control the novel established preclinical drug testing approach, and to assure, that the results are trustworthy, a classical preclinical trial was performed. Here, ALL-265 cells were injected into mice, which should be sensitive to venetoclax according to the multiplex *in vivo* trial. Mice were treated and analysed as in the multiplex trial, except that no mice for the time point therapy start were injected.

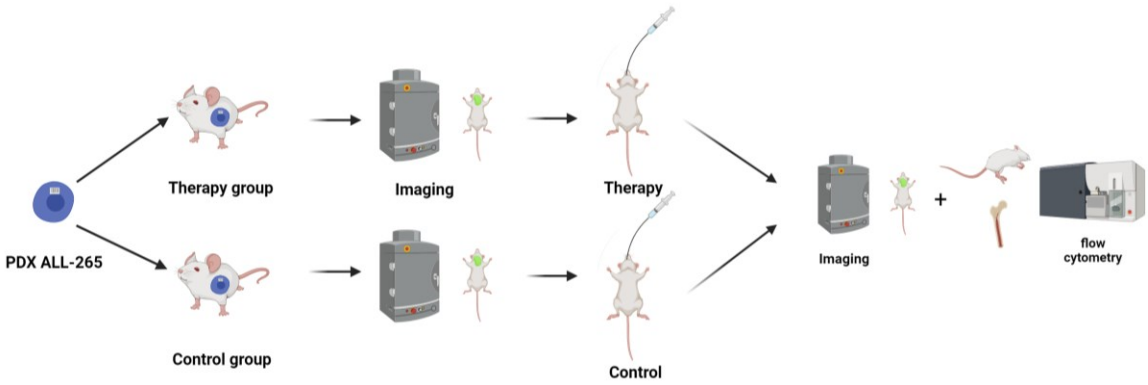

Figure 9. Experimental set up for a classical preclinical trial in ALL-265

Experiment was performed as described in Figure 7, except that only ALL-265 cells were injected into mice, and no therapy start group was required.

ALL-265 cells were thawed and injected into groups of mice. After 21 days, mice were treated for 2.5 weeks with venetoclax or solvent control. Tumour burden was quantified by bioluminescence imaging. As expected, tumour burden of venetoclax-treated mice was reduced compared to control mice (figure 10A). Body weight was stable during the study (figure 10B).
For post mortem analysis, PDX cells were re-isolated from murine bone marrow as described.
A significant reduction of human cells in the venetoclax treated mice in bone marrow (figure 10C) could be observed. Furthermore, both spleen weight and spleen size were reduced in the treated group (figure 10D). These data imply a sensitivity of ALL-265 cells towards venetoclax.
Taken together, the response of ALL-265 towards venetoclax was similar in the classical preclinical trial compared to the multiplex *in vivo* trial. Furthermore, I was able to demonstrate the consistency of a classical preclinical trial with the novel multiplex *in vivo* assay in ALL. This implies the further use of the approach and reduces mouse numbers.

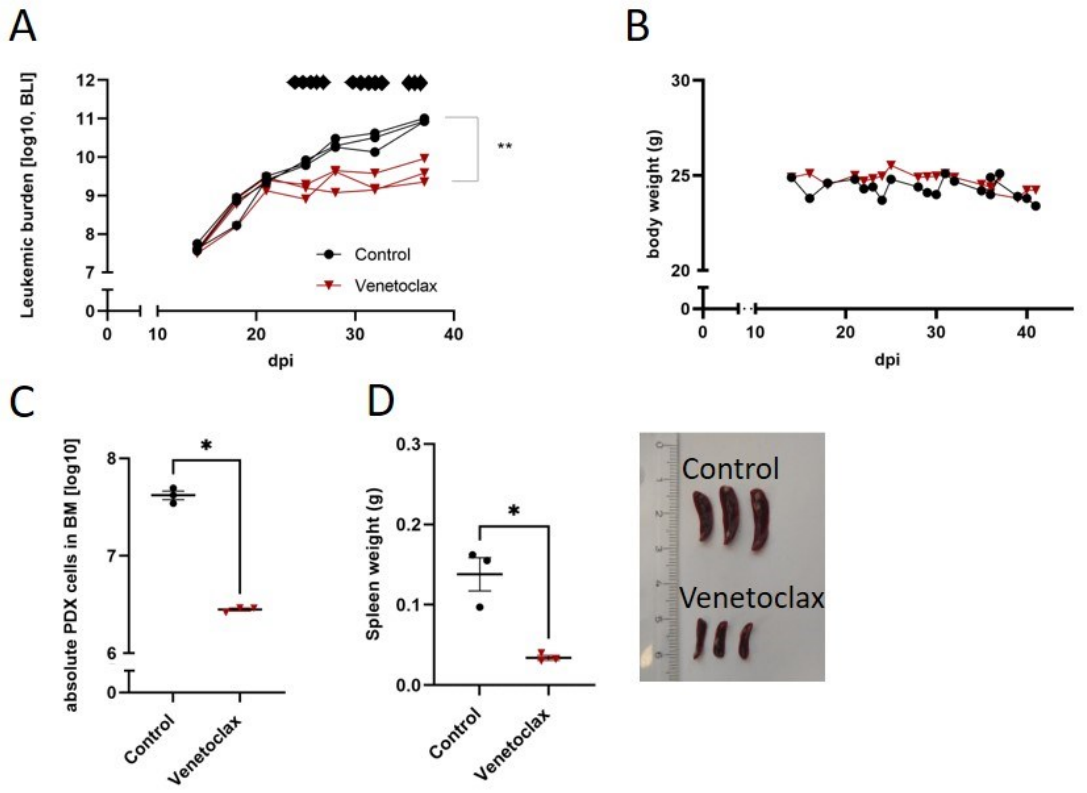

Figure 10. Targeting *BCL2* with venetoclax in ALL-265.

Experiment was performed as described in figure 9.

a.Bioluminescence *in vivo* imaging of control (n=3; black) and treated (n=3;red) mice (p=0.0017 by Welch t-test); diamonds indicate days of therapy b. Body weight of mice during therapy (mean). c-d. After 2.5 weeks of treatment, all mice were sacrificed and BM cells isolated. Absolute number of human cells in BM c. was measured in flow cytometry. Each dot represents one mouse. Mean ± SEM is shown; Statistical analysis was performed by Welch t-test: p= 0.0119 d. Spleen weight was measured. Mean ± SEM is shown (left; p=0.0346 by Welch t-test). Spleen size was determined (right).

5.4.3. Targeting *MCL1* with S63845 identified two sensitive ALL samples

The molecular *in vivo* screen revealed a dependency of *MCL1* in three ALL samples (ALL-50, ALL-199 and ALL-502), suggesting a putative response in these samples towards an inhibition of the anti-apoptotic protein, while two samples might be resistant. Therefore, a preclinical trial with the specific MCL1 Inhibitor S63845 was conducted.

As in previous experiments cells were mixed and transplanted into groups of mice. Mice were in a good condition and showed physiological behaviour. Unfortunately, one mouse did not engraft and was excluded from the trial. One mouse engrafted slower and was included in the trial one week later. Five mice were sacrificed and analysed at start of therapy time point. Flow cytometry data depicts homogeneous engraftment (figure 11F). The other groups of mice were treated with either S63845 or solvent as control.

At the beginning of the study, the body weight was constant, but during the therapy, the control group constantly lost weight, while the treated group had a rather constant weight with minimal deviations (figure 11E).

Five to six days after the last dose, mice were sacrificed and analysed. In this study, the bioluminescence imaging signal did not show a reduction in treated compared to control mice (figure 11A,11B). Accordingly, no significant difference for the spleen weight and the human cells in bone marrow was

ascertained (figure 11C, 11D). These data indicate that the bulk of ALL PDX cells showed no response towards S63845.
In bone marrow, the absolute numbers of ALL-50 and ALL-199 showed a reduction of leukemic cells in S63845 treated mice compared to control, while cells of ALL-265, ALL-502 and ALL-1034 were not altered. These data indicate that S63845 might inhibit cell growth in ALL-50 and ALL-199, but does not affect ALL-265, ALL-502 and ALL-1034 cells (figure 11F).
When comparing therapy start with S63845 treated mice, it became obvious that all samples showed an increase in tumour cell burden even under therapy, albeit reduced compared to solvent control mice (Figure 11F).
Overall, this experiment revealed the sensitivity of two PDX samples and resistance of three PDX samples towards the targeting drug S63845.

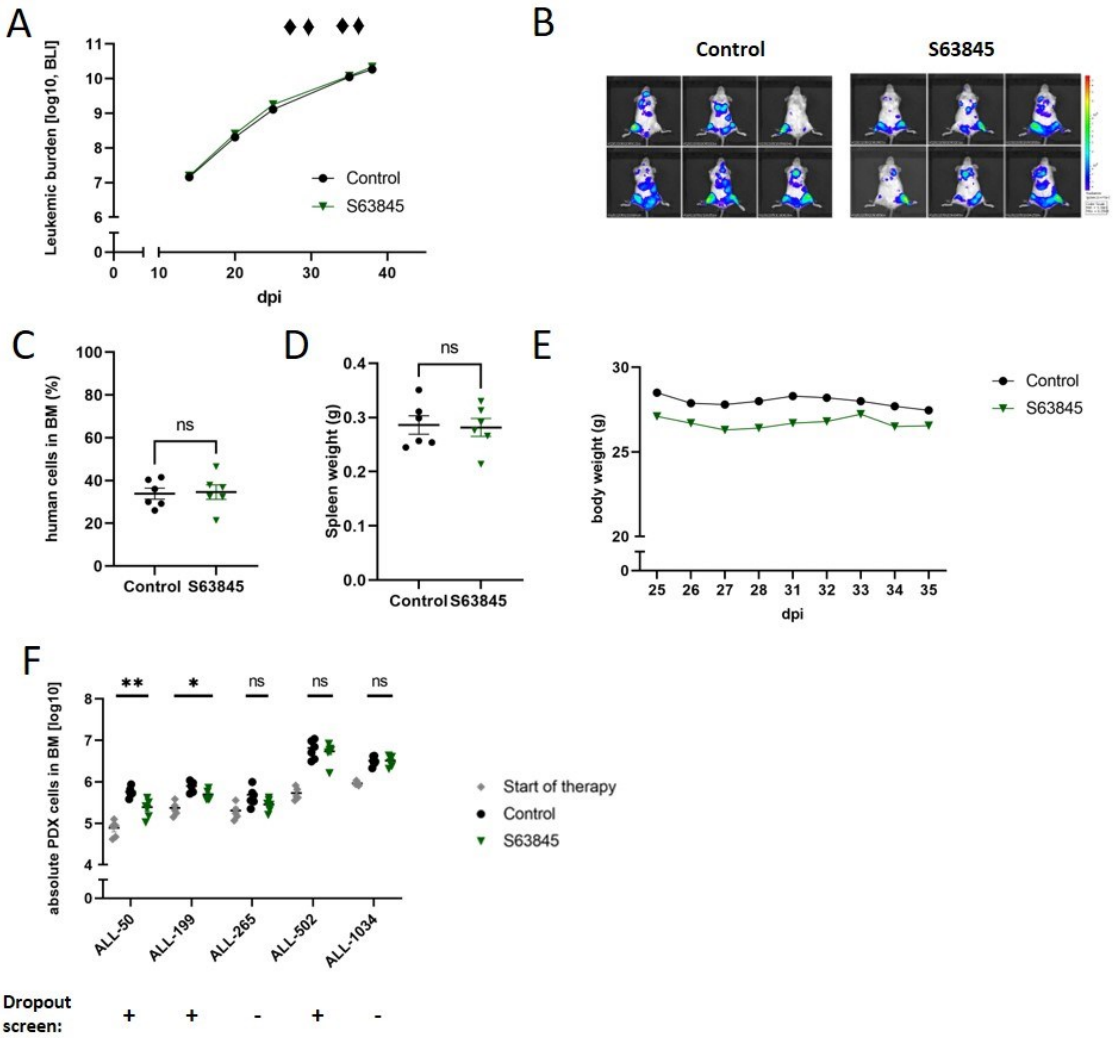

Figure 11. Targeting *MCL1* with S63845 using the multiplex *in vivo* assay

Experiment was performed as described in figure 7. Mice were treated with four doses of S63845 (25 mg/kg i.v.; n=6; green) or solvent as control (n=6; black). Mice were sacrificed on day 39/40 after injection.

a. Quantification of bioluminescence *in vivo* imaging signals of control (n=6) and treated mice (n=6 diamonds indicate days of therapy b. and individual pictures on day 38 after injection c. Percentage of human cells present in bone marrow (BM) in control and treated mice on day 39/40 (mean ± SEM, p= 0.8714 by Welch t-test) d. Spleen (SPL) weight of control and treated mice on day 39/40 (mean ± SEM , p= 0.8531 by Welch t-test) e. Body weight of mice during therapy (mean). f. Analyses depicting each PDX population. Absolute cell numbers for each sample is indicated for BM. Comparison of mice time point start of therapy (grey) with control (black) and treated mice (green). Each dot represents one mouse. Mean ± SEM is shown. Statistical analysis was performed by Welch t-test: ALL-50: p=0.0028, ALL-199: p=0.0257, ALL-265: p=0.1321, ALL-502: p=0.5176, ALL-1034: p=0.9804 by Welch t-test.

5.4.4. Targeting *XPO1* with eltanexor displayed four sensitive ALL samples

The molecular *in vivo* screen revealed a dependency for *XPO1* in all five ALL samples. To target *XPO1 in vivo*, the specific XPO1 inhibitor eltanexor (KPT-8602) was chosen.
Experiment was performed as described (see 5.4.1; 5.4.3). When leukaemia developed a defined leukaemia burden in bioluminescence imaging start of therapy mice were sacrificed and analysed to examine the distribution between the populations within a mouse as described earlier. All populations engrafted similarly, as depicted in figure 12F. All mice showed physiological behaviour and a good body condition during therapy.
The other groups of mice were treated for 2 weeks with either eltanexor or solvent as control. Four to five days after the last dose, mice were sacrificed and analysed.
The bioluminescence imaging signal was significantly reduced in treated compared to control mice (figure 12A;12B). Accordingly, the total amount of human cells in the bone marrow, i.e. the amount of five PDX samples, was reduced in the treated mice compared to control mice (figure 12C). Furthermore, a significant reduction of the spleen weight was observed (figure 12D). These data suggest a putative sensitivity of ALL PDX cells towards eltanexor.
A minimal body weight loss was observed. Only one mouse (86022) fluctuated with weight, which improved in the second week of therapy again (figure 12E)
Notably, the absolute numbers of leukemic cells from ALL-50, ALL-199, ALL-265, and ALL-1034 showed a drastic decrease in tumour burden in eltanexor compared to control treated mice in bone marrow. Amount of ALL-502 cells, was unchanged under therapy in bone marrow (figure 12F).
When comparing therapy start with eltanexor treated mice, clear reduction of leukemic cell count was observed in ALL-199 and ALL-265; for ALL-50 and ALL-1034, number of cells was similar at both time points (figure 12F). These data indicate that eltanexor might cause cell death in ALL-199 and ALL-265, inhibits cell growth in ALL-50 and ALL-1034, and does not affect ALL-502 cells.
In Conclusion, four of five PDX samples were sensitive towards the XPO1 inhibitor eltanexor, whereas one PDX sample was resistant.

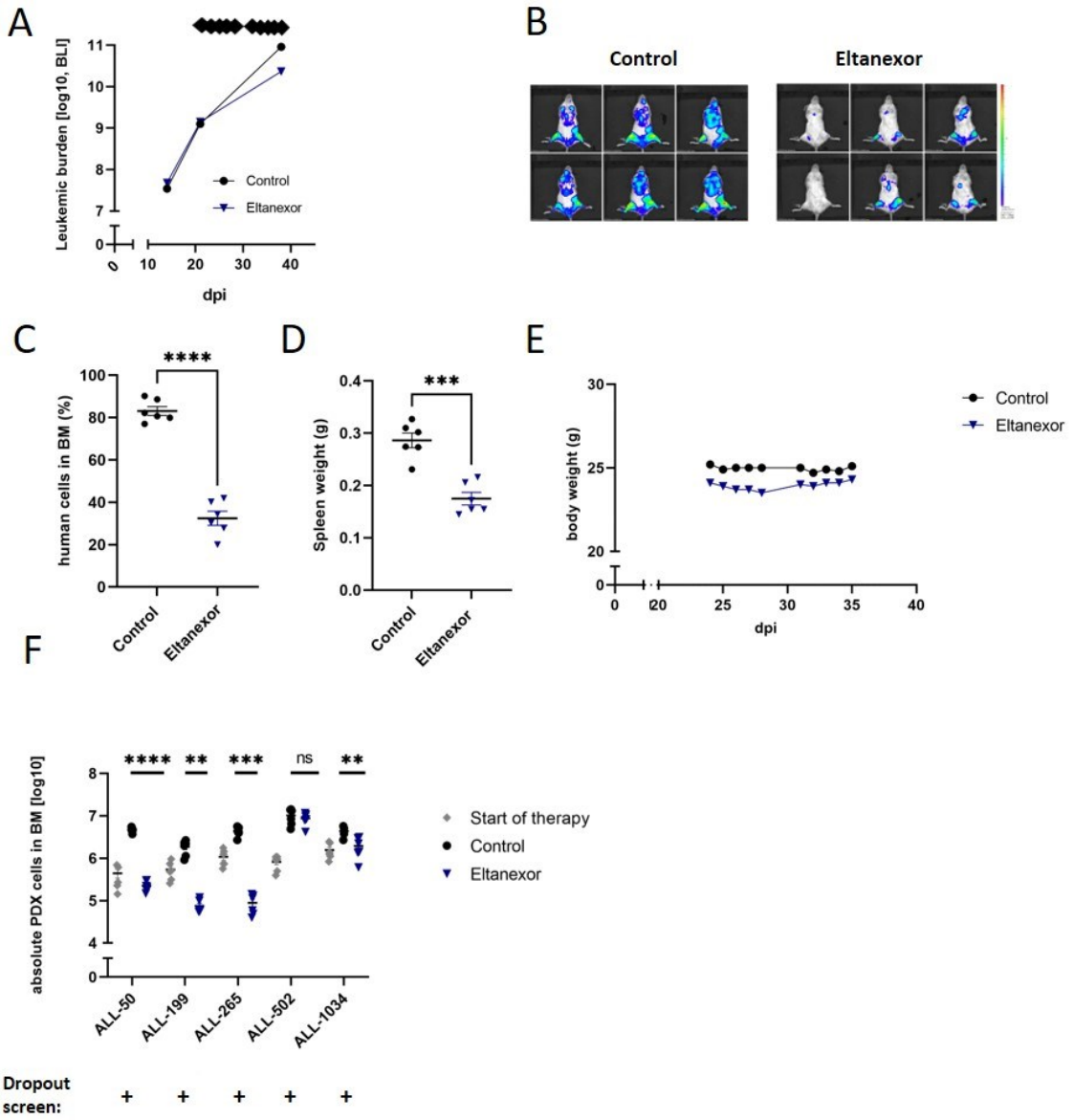

Figure 12. Targeting XPO1 with eltanexor using the multiplex *in vivo* assay

Experiment was performed as described in figure 7. Mice were treated with ten doses of eltanexor (15 mg/kg p.o.; blue) or solvent as control (black). Mice were sacrificed on day 39/40 after injection.

a.Quantification of bioluminescence *in vivo* imaging signals of control (black) and treated mice (blue), diamonds indicate days of therapy b. and individual pictures day 38 after injection c. Percentage of human cells present in bone marrow (BM) in control and treated mice on day 39/40 after injection (mean ± SEM, p= 0.0001 by Welch t-test) d. Spleen (SPL) weight of control and treated mice on day 39/40 after injection (mean ± SEM , p=0.0133 by Welch t-test) e. Body weight of mice during therapy (mean).

f. Analyses depicting each PDX population. Absolute cell numbers for each sample is indicated for BM. Comparison of mice time point start of therapy (grey) with control (black) and treated mice (blue). Mean ± SEM is shown. Statistical analysis was performed by Welch t-test: ALL-50: p=<0.0001, ALL-199: p=0.0015, ALL-265: p=0.0002, ALL-502: p=0.4750, ALL-1034: p= 0.0049 by Welch t-test.

5.5. Sample-specific correlation between molecular dependency and treatment response towards the respective drug

After conducting preclinical trials, pharmacological response was analysed and compared to results from molecular dropout screens performed by Diana Amend.
The CRISPR/Cas9 screen revealed a dropout of *BCL2* in ALL-50, ALL-199, ALL-265 and ALL-502, whereas ALL-1034 did not show a dependency on *BCL2*. Therefore, we hypothesised that the first four samples should response towards a BCL2 inhibitor, while the latter one should be resistant. In line with this prediction, the therapy trial displayed a sensitivity towards venetoclax in ALL-50 and ALL-265, and a resistance in ALL-1034. For ALL-199 and ALL-502, however, the results from molecular and pharmacological trials did not match. For *BCL2*, the molecular-functional results correlated with the drug-functional results in three out of five samples (figure 8, table 15).
As second target, the molecular *in vivo* screen revealed a dependency towards *MCL1* in three ALL samples (ALL-50, ALL-199 and ALL-502); however, only ALL-50 and ALL-199 responded towards the inhibitor, while ALL-502 did not. ALL-265 and ALL-1034 were resistant towards the MCL1 inhibitor as predicted by the screen. Therefore, the molecular-functional results correlated with the drug-functional result in four out of five samples (figure 11, table 15).
Finally, *XPO1* was detected as a putative dependency in all five samples; of those only four responded towards the XPO1 inhibitor (ALL-50, ALL-199, ALL-265 and ALL-1034). In summary, four of five molecular-functional results correlated with the drug-functional results (figure 12, table 15).
Of note, prediction accuracy differed between the samples; while the results of molecular screen and treatment trial correlated in three of five PDX samples for all three tested target/drug pairs (ALL-50, ALL-265, ALL-1034), one sample showed a positive correlation only for two target/drug pairs (ALL-199), and one sample revealed no correlation at all (ALL-502).
In summary, a high correlation between molecular-functional and drug-functional results was possible in three of five samples. Further experiments are needed to understand why the two functional tests did not correlate at all for one tested sample.

	ALL-50	ALL-199	ALL-265	ALL-502	ALL-1034
***BCL2* dropout**					
Response venetoclax					
***MCL1* dropout**					
Response S63845					
***XPO1* dropout**					
Response Eltanexor					

Table 15. Correlation of molecular dropout screens with pharmacological therapy trials
Green: dropout/ drug response; Red: no dropout/no drug response.

6. Discussion

Approaches to identify a biomarker for precision medicine remains challenging, still they are necessary to allocate patients to individualised, targeted therapies. Targeted therapies are required, due to the insufficient effectivity of conventional chemotherapy resulting in severe side effects and relapse (BAGNYUKOVA et al., 2010). Even though cure rates in ALL are improving, relapse remains challenging and results in poorer outcome, highlighting the need for novel treatment options (MULLIGHAN et al., 2008; SALVARIS & FEDELE, 2021). Until today, the usage of targeted therapies in ALL is rather minor, since only BCR::ABL inhibitors or immunotherapeutics targeting CD19 or CD22 are FDA approved, compared to other leukaemia entities, such as CLL or AML.

In this study, the aim was to establish a molecular-functional approach in order to identify individual biomarkers and thereby define suitable drugs for individualised therapy. I tested the effect of selected targeted therapies *in vivo* and correlated the results with data from molecular CRISPR/Cas9 screens. Testing targeted therapies revealed the prediction accuracy of dropout screens. Furthermore, I established a novel preclinical drug testing approach for ALL using colour marked PDX samples. The multiplex *in vivo* assay allows simultaneous testing of up to five PDX samples. The usage of this approach resulted in a reduction of mice by a factor five. This approach was successfully used to test selected targeted therapies against defined PDX ALL models *in vivo*.

6.1. Molecular and functional approaches using PDX cells can define biomarkers

Within the last decades and years, several molecular and functional approaches have been established to identify individual biomarkers to facilitate effective individualised treatment for cancer patients. While some approaches have already entered clinical routine, others are still in development.

Patients who present at the clinics with leukaemia-related symptoms undergo a haemato-pathological examination to diagnose leukaemia. Today, cytogenetics and molecular cytogenetics are part of the standard protocol as described (see 1). Conventional cytogenetics has its limitations in the insufficient quality of metaphases in leukemic cells, which can affect the characterization of chromosomal breakpoints. Conventional cytogenetics was then optimized by molecular cytogenetics, e.g. FISH, in which the detection of specific known nucleic acids takes place at the chromosomal level using specific probes. FISH is widely used to detect patients harbouring BCR::ABL translocation and these patients are assigned to BCR::ABL inhibitors, e.g. imatinib. (AVET-LOISEAU, 1999; BROWN et al., 2020)

Karyotyping is used to detect chromosomal changes, but only up to a limited copy numbers size, which might be clinically relevant too (CUPPEN et al., 2022). However, these methods only allow a limited prediction of treatment options and the combination with limited available treatment options complicates the treatment. While there are many drugs existing, the biomarker to link the needed drug to the patient is not yet available.

To circumvent the limitations of conventional and molecular cytogenetics, tumour material is sequenced on a genome and exome basis, as well as transcriptional profiling and copy number determination at the chromosome level to match patients to individualised treatment. (WORST et al., 2016; VAN TILBURG et al., 2021). Especially ALL patients are often underrepresented in these trials, whereas for AML e.g. the BEAT AML study exists (BURD et al., 2020). This might be due to the fact, that ALLs are mainly characterised by translocations and chromosomal aberrations compared to AML, which has a strong focus on mutations. However, these approaches are only based on descriptive data; therefore, a mere pre-selection is possible. In addition, genomic analyses are often insufficient to assign patients to matching treatment schemes, since retrospective studies identified a low response towards

current existing targeted therapies (PRASAD, 2016; MARQUART et al., 2018). These data highlight the need for novel therapies, because many targets would be 'druggable', but matching inhibitors are still missing (JIANG et al., 2022). Furthermore, these techniques are expensive and time-consuming, making it difficult for clinicians to apply the acquired datasets in the clinic.

Ex vivo drug testing is another tool for precision medicine. Patient primary material gets screened with a customized drug library and helps to assign patients to the targeting treatment scheme they could profit from (PEMOVSKA et al., 2013; ROIFE et al., 2016; SPINNER et al., 2020; MALANI et al., 2022). This enables rapid testing of a large number of drugs in short time. There are already drug compound libraries for *ex vivo* approaches on the market, unfortunately, they are still restricted to research use. To my knowledge, there are currently no primary ALL tests used in the clinics (WANDER et al., 2022); however, *ex vivo* drug tests have already been performed on primary AML cells and patients subsequently assigned to appropriate treatments (MALANI et al., 2022). In the study of Malani and colleagues, results were promising and therefore current compound drug libraries restricted to research use, have a potential to be used in clinical trials in the future. However, primary samples show an altered proliferation *ex vivo* compared to *in vivo,* which may influence the results (NIJMEIJER et al., 2001; MITRA et al., 2013). Another drawback of *ex vivo* assays for haematological samples is the missing interaction with the niche and the bone marrow microenvironment and could be the reason for discrepancies seen *in vivo* (EBINGER et al., 2016; HOUSHMAND et al., 2019). In addition, we know from our own unpublished data, that especially ALL samples are technically difficult to keep in culture.

To overcome the drawbacks from established techniques for predicting drug response of individual patient samples, we aimed to establish a molecular-functional approach in order to identify individual biomarkers and thereby define suitable drugs for individualised therapy. As a model system, we work with PDX cells. To establish and work with a PDX model, primary cells have to be transplanted into immunodeficient mice to avoid graft rejection; both the lack of immune cells and the differences between a murine and human bone marrow niche may influence the preclinical treatment trials. Humanised mouse models are being developed to enable a better interaction with the tumour microenvironment. Several studies have shown, that murine stroma can replace the human tumour stroma across mice strains, and thus might influence our scientific objective, too. (RICHMOND & SU, 2008; SIOLAS & HANNON, 2013; HIDALGO et al., 2014; SAJJAD et al., 2021)

Despite an altered microenvironment and absent immune system, the xenograft model is superior to the use of cell lines, since it enables the modelling of the complexity of primary tumours. Cell lines, show molecular and cellular deviations after prolonged culture and passaging compared to primary patient cells and PDX cells (PAN et al., 2009; SCHUELER et al., 2018; KUWATA et al., 2019). Since primary patient cell material is limited and cells face decomposition and viability loss, it makes it difficult to perform prolonged experiments *ex vivo* (MEIJER et al., 2017). Therefore, usage of the PDX models allows to amplify patient material and thereby facilitates repetitive and reproducible *in vivo* and *ex vivo* experiments. Consequently, multiple analyses, e.g. molecular and functional assays, can be performed from material obtained from individual patients.

Meanwhile, a variety of established ALL PDX models are existing and successfully mimic the biology and of leukaemia in immunodeficient mice (KAMEL-REID et al., 1989; BORGMANN et al., 2000; LOCK et al., 2002; LIEM et al., 2004; TERZIYSKA et al., 2012; TOWNSEND et al., 2016). It has been shown that PDX models retain characteristics of primary ALL patient cells (SCHMITZ et al., 2011; CASTRO ALVES et al., 2012) making them attractive for the usage for preclinical treatment trials. However, selection for certain cells, especially aggressive sub clones, takes place, which can be seen from the second PDX passage onwards (MEYER & DEBATIN, 2011; SCHMITZ et al., 2011). Dependent on engraftment time, insights can be gained within a few weeks. On the other hand, engraftment time and engraftment failure are a major challenge in establishing a PDX model

(HIDALGO et al., 2014). Here, we pre-selected for highly aggressive PDX samples with a fast engraftment (<50 days).

Today, PDX models are widely used for preclinical treatment trials (LOCK et al., 2002; TOWNSEND et al., 2016; WIRTH et al., 2022). In an intertwined project performed by Diana Amend in the group, CRISPR/Cas9 dropout screens were performed to identify putative biomarkers for individual PDX samples. These screens revealed molecular dependencies on an individual basis. The aim of this project was to determine if these molecular dependencies correlate with drug response in preclinical treatment trials.

6.2. Marking individual PDX samples with fluorochromes enables a novel preclinical drug testing approach for ALL

Before clinical application, novel therapies require preclinical testing according to the FDA and the German Medical Products Act. Preclinical testing approaches are resource intensive considering mice, manpower and economics. Xenograft mouse models are well established for preclinical testing of chemotherapies (LOCK et al., 2002; LIEM et al., 2004; EBINGER et al., 2016; WIRTH et al., 2022) as well as for targeted therapies (GAO et al., 2015; POMPILI et al., 2016; TOWNSEND et al., 2016; LAU et al., 2022). In order to test selected targeted therapies *in vivo*, I aimed to increase the efficiency of preclinical testing.

From primary patient material, PDX mouse models of ALL, which allow serial transplantation in immunodeficient NSG mice, were established, and five ALL PDX samples with different molecular alterations, but similar *in vivo* growth behaviour, were selected for the multiplexing approach. Reliable transplantation is necessary to evaluate the response to the drug correctly, and serial transplantation is necessary to genetically modify the cells. PDX cells were labelled with unique fluorochromes to later on distinguish between populations in a single mouse. Marking cells with a fluorochrome is a known tool to study cell clonality (WEBER et al., 2011; ZELLER et al., 2022) and is used for competitive *in vivo* approaches in the hosting laboratory (CARLET et al., 2021; GHALANDARY et al., 2022). In this approach, I used unique labelled PDX samples and injected a mix of five samples into groups of mice. For post mortem analysis, PDX cells were re-isolated from murine bone marrow and absolute tumour burden of PDX cells was quantified by flow cytometry. Determining the abundance of five fluorochromes allowed quantifying the amount of cells, that each of the five samples contributed to the entire tumour load. (HUNT et al., 2022)

In the first mixing experiment, I detected growth discrepancies for some PDX samples and no increase in leukemic cells was observed from the first time point to the end of the experiment. One sample was overrepresented in the mix, and it might be that this sample repressed the growth of the other samples and thereby might influence the results (see 5.3.1). In order to ensure a reliable evaluation of the trials, another kinetic trial with an adjusted mixture was performed. Here the overrepresented sample was given a disadvantage and the other samples and their growth increase were equally detectable by flow cytometry (see 5.3.2). In summary, mixture adjustment is required to ensure a reliable evaluation of preclinical trials using the multiplex *in vivo* assay. A study from our laboratory, which published the first multiplex approach with five individual PDX samples, includes a sample which received an advantage due to slower engraftment, highlighting the importance of a known mixture (WIRTH et al., 2022). The quality control (see 5.4.2) demonstrated that the samples do not enhance each other and therefore results are rated as reliable.

Since no sequencing is required for fluorochrome labelled cells, mice can be analysed immediately after terminating treatment. Furthermore, if technical problems with equipment occurs, cells can be viable frozen and measured at a later time point. On the other hand, loss of viable cells due to freezing and

thawing should be considered. This would not affect the relative composition, but the absolute numbers of human cells. Nevertheless, this preclinical testing approach is limited to a number of samples that can be used, due to limited amount of fluorochromes and colour panel settings. Whereas marking cells with individual barcodes do not face a number limitation, but a more complex read out, including a PCR and further sequencing, which is time consuming. To my knowledge, no similar preclinical treatment studies have been published, besides the study of Wirth et al.

With this approach, I was able to reduce the amount of mice in line with the 3R concept as appealed by Russell and Burch (RUSSELL & BURCH, 1959). I correlated three genes in five PDX samples with a sum of 54 mice (3 trials with 3 groups and 6 mice per group). Without the multiplex *in vivo* assay, a total amount of 180 mice would have been needed (3 trials with 5 individual samples with 2 groups and 6 mice per group). As individual samples can be followed by BLI in our lab, no start of therapy group is needed in trials without multiplexing, which results in two instead of three groups compared to the multiplex *in vivo* assay. However, establishment of cells labelled with fluorochromes required 12 additional mice, as well as the kinetic trial to optimize mixing conditions. Consequently, the sum of mice needed (n=85) used for establishment (n=31) and conduction of multiplex trials (n=54) is still less than half of the number of mice needed in a classical preclinical trial. The establishment was resource intensive, too; however, from now on it is a valuable tool for further preclinical treatment trials. I assume that this is an improvement for preclinical testing.

Taken together, I successfully established a novel preclinical testing approach for ALL PDX samples. With this promising approach, I was able to determine the efficacy of three targeted drugs on five individual samples in parallel, which reduced the resources by factor five. This approach is a valuable tool to perform further preclinical treatment trials, independently of a correlation with CRISPR/Cas9 screens.

6.3. Biomarkers identified by molecular screens correlate with drug response in most tested samples

Diana Amend identified three genes that showed a dropout in at least two patient samples. I then performed *in vivo* therapy trials to understand if results from dropout screens correlate with drug response. As a certain correlation is given, screens were used as a biomarker to predict drug response.

One gene that showed a dropout in four out of five ALL PDX samples was *BCL2* (see 5.1.1). As mentioned in 1.4.3.1 the overexpression of BCL2 is known in haematological malignancies (COUSTAN-SMITH et al., 1996; ROBERTSON et al., 1996; ROBERTS et al., 2021). Pharmacological response towards venetoclax correlated with the CRISPR/Cas9 screen in three out of five cases. One explanation might be that the cellular effects of a knockout are much stronger than a pharmacological inhibition. Furthermore, the effects of the knockout were analysed after 5-6 weeks of growth in mice, while treatment only lasted for two weeks. I assume that patients could profit most from a specific BCL2 inhibitor if the drug also reduces tumour burden as in samples ALL-50 and ALL-265 (see figure 8F). But also, the patient ALL-1034 may benefit from the screening approach, as they would have been immediately ruled out for a BCL2 inhibitor and could have been allocated to other specific targeted treatments.

The CRISPR/Cas9 screen yielded *MCL1* as a dependency in three out of five PDX samples. *MCL1* has a high oncogenic potential and counts to the anti-apoptotic BCL2 family proteins as *BCL2*. *MCL1* is known to be highly expressed in haematological malignancies (GORES & KAUFMANN, 2012; WANG et al., 2021). To target *MCL1* pharmacologically *in vivo*, PDX samples were treated with the specific MCL1 inhibitor S63845 (KOTSCHY et al., 2016). The correlation highlights that the

CRISPR/Cas9 screen was able to predict the response and resistance towards a MCL1 inhibitor in four out of five PDX samples. Again, ALL-502 was resistant, contrary than predicted by the screen.

Importantly, intensity of the response in the sensitive samples was minor and may not be clinically relevant, strengthening the assumption that the knockout is too strong and the drug response is overestimated. An increase of the drug dose might result in a stronger response. However, due to legal limitations, our laboratory is only allowed to test published concentrations. Moreover, a stronger effect could be achieved when combining venetoclax and S63845, as successfully demonstrated in T-ALL cell lines and xenograft models of B-ALL (LI et al., 2019; MOUJALLED et al., 2020; SEYFRIED et al., 2022). Furthermore, patients with a dropout of *MCL1* could benefit from a treatment regimen combining S63845 and conventional chemotherapy, as it has been demonstrated, that inhibiting of anti-apoptotic proteins can strengthen the effect of conventional chemotherapy (POTTER et al., 2021).

It is striking that two genes of the BCL2 family were detected as dependencies. Here, BH3 profiling would have been an option to detect *BCL2* and *MCL1,* too. BH3 profiling is based on the binding of BH3 peptides to BCL2 family proteins involved in the regulation of apoptosis and measures apoptosis induction (DENG et al., 2007). Seyfried and colleagues were able to demonstrate an association between high *BCL2* gene expression and a strong response towards venetoclax *ex vivo* and *in vivo*, while high expression at the transcript and protein level was not associated with a strong response to the drug. A major advantage of BH3 profiling is, that no cultivation of primary cells is required, only a small number of cells is needed, non-invasive cell gaining is sufficient, and results can be available within a few hours. (SEYFRIED et al., 2019; MANZANO-MUNOZ et al., 2022) Therefore, BH3 profiling could be a valuable biomarker for clinicians to guide the use of BH3 mimetics, such as venetoclax or S63845.

XPO1 is another dependency revealed through the CRISPR/Cas9 drop out (see 5.1.1). In order to correlate results from the preclinical trials with the CRISPR/Cas9 screen *in vivo*, a study with the XPO1 inhibitor eltanexor was conducted (see 5.4.4). Four of five PDX samples were sensitive towards the XPO1 inhibitor, with a clear drop in tumour burden in three of the sensitive samples. Here, the intensity of response towards eltanexor differed between the samples. Again, ALL-502 was the sample where screen results did not correlate with the preclinical data. As mentioned above, a possible treatment schedule for ALL-502 could be conventional chemotherapy in combination with eltanexor. Eltanexor is currently only tested in one clinical trial, recruiting AML patients among other neoplasia's (NCT02649790). My and other groups data showed efficacy of eltanexor in preclinical ALL cells (VERCRUYSSE et al., 2017; GOVAERTS et al., 2021); consequently, I see a strong potential for ALL patients and more investigation towards clinical trials with ALL patients is needed.

The leukaemia of patient ALL-502 might be a particularly severe form of leukaemia since it engrafts faster (see 5.3.1). This sample is striking in all preclinical trials conducted in this study. It can be discussed, that ALL-502 already reached its leukemic plateau in bone marrow when therapy starts. Therefore, an earlier time point of treatment would be needed. On the other hand, this is not in line with our own unpublished BLI data. Therefore, I conclude that the knockout is too strong and overestimates the efficacy of a drug. Vice versa, this states the importance for the need of even more specific drugs.

Taken together, the correlation of preclinical studies with CRISPR/Cas9 screen data revealed that the dropout is stronger than a drug. Consequently, this resulted in an overestimation of the drug efficacy. However, the results of the present study highlight that the CRISPR/Cas9 screens can predict a drug response on an individualised basis, but not the intensity of response. Here, the importance of individualised precision medicine is strengthened by the screen, since the PDX samples displayed different dependencies and heterogeneous response towards drugs. However, we have not yet tested this approach on primary patient cells, so it is difficult to compare our approach with those routinely used in the clinic.

Using CRISP/Cas9 screens, genes were identified on a patient-individual basis. These individual dependencies were addressed with specific inhibitors, and in the further course, it would be interesting to see whether these inhibitors can sensitise the cells towards conventional chemotherapy.
Due to the limitation that the intensity of the drug response cannot be predicted, an optimisation of the CRISPR/Cas9 screens might be required, e.g. shortening the time for read-out, so that the intensity would be predictable. This was not part of the project, but could be interesting for future studies. In addition, the specificity of targeted drugs needs to be optimised.

7. Summary

Establishing multiplex *in vivo* assays in a xenograft mouse model of acute leukaemia to correlate preclinical treatment trials with molecular screens

Acute leukaemia is a rare disease, but the number of cases reported each year is steadily increasing. Standard therapy includes classical chemotherapy, which most patients respond to at the beginning. However, a major problem is relapse, which is associated with a poorer prognosis, so better treatment options are urgently needed.

With advances in sequencing technology, more and more molecular features can be identified. As a result, patients benefit from more specific diagnostics and can be matched to potential specific treatment options. The number of targeted inhibitors has been increasing for years, and while there are many drugs existing, the biomarker to link the needed drug to the patient is not yet available.

In the present study, the results of molecular dropout screens were used as a basis. The aim of the present study was to test the effect of selected targeted therapies against five PDX ALL models with different molecular alterations. Specific inhibitors were used to determine whether the molecular screen could predict a response to an inhibitor and results were correlated with the existing data from molecular screens.

In order to preclinically test novel therapies, this work aimed to increase the efficiency of preclinical therapy trials. I was able to establish a multiplex protocol for *in vivo* treatment trials, allowing up to five ALL-PDX samples to be tested simultaneously in competitive *in vivo* trials. Flow cytometry was used to detect individual samples and investigate response towards targeting drugs. With this method, I was able to test three targeted therapies *in vivo*, while reducing the required number of mice by a factor of five, in line with the 3R concept.

Detected dependencies *in vivo* were *BCL2, MCL1* and *XPO1*. The correlation of *in vivo* therapy trials with the molecular functional results was high, with a positive correlation in three of five samples for all tested target / drug pairs, one sample with two positive correlations, and only one sample with no correlation between the two independent approaches. However, the PDX samples responded differently to the specific inhibitors, which highlights the concept of personalised medicine. Furthermore, the results state that the screen overestimates the efficacy of the drug.

8. Zusammenfassung

Etablierung von Multiplex *in vivo* Tests in einem Xenograft-Mausmodell für akute Leukämie zur Korrelation von präklinischen Behandlungsversuchen mit molekularen Screens

Die akute Leukämie ist eine seltene Krankheit, aber die Zahl der jährlich gemeldeten Fälle nimmt stetig zu. Zur Standardtherapie gehört die klassische Chemotherapie, auf die die meisten Patienten zu Beginn ansprechen. Ein großes Problem sind jedoch Rückfälle, die mit einer schlechteren Prognose verbunden sind, so dass dringend bessere Behandlungsmöglichkeiten benötigt werden.

Mit den Fortschritten in der Sequenzierungstechnologie können immer mehr molekulare Merkmale identifiziert werden. Infolgedessen profitieren die Patienten von einer spezifischeren Diagnostik und können auf mögliche spezifische Behandlungsoptionen abgestimmt werden. Die Zahl der zielgerichteten Inhibitoren nimmt seit Jahren zu, und obwohl es bereits viele Medikamente gibt, ist der Biomarker, der das benötigte Medikament dem Patienten zuordnet, noch nicht verfügbar.

In der vorliegenden Studie wurden die Ergebnisse von molekularen Dropout-Screens als Grundlage verwendet. Ziel der vorliegenden Studie war es, die Wirkung ausgewählter zielgerichteter Therapien gegen fünf PDX-ALL-Modelle mit unterschiedlichen molekularen Veränderungen zu testen. Es wurden spezifische Inhibitoren verwendet, um festzustellen, ob die Screens ein Ansprechen auf einen Inhibitor vorhersagen können und die Ergebnisse wurden mit den vorhandenen Daten aus molekularen Screens korreliert.

Um neuartige Therapien präklinisch zu testen, zielte diese Arbeit darauf ab, die Effizienz von präklinischen Therapieversuchen zu erhöhen. Es gelang mir, ein Multiplex-Protokoll für *in vivo* Behandlungsversuche zu entwickeln, mit dem bis zu fünf ALL-PDX-Proben gleichzeitig in konkurrierenden *in vivo* Versuchen getestet werden können. Mittels Durchflusszytometrie konnten die individuellen Proben erkannt werden und das Ansprechen auf die Medikamente bestimmt werden. Mit dieser Methode konnte ich drei zielgerichtete Therapien *in vivo* testen und gleichzeitig die Anzahl der benötigten Versuchsmäuse um das Fünffache reduzieren, ganz im Sinne des 3R-Konzepts.

In vivo wurden Abhängigkeiten für *BCL2, MCL1* und *XPO1* festgestellt. Die Korrelation der *in vivo* Therapieversuche mit den molekularen funktionellen Ergebnissen war hoch, mit einer positiven Korrelation in drei von fünf Proben für alle getesteten target-drug Paare, einer Probe mit zwei positiven Korrelationen und nur einer Probe ohne Korrelation zwischen den beiden unabhängigen Ansätzen. Allerdings sprechen die PDX-Proben unterschiedlich auf die spezifischen Inhibitoren an, was das Konzept der personalisierten Medizin unterstreicht. Außerdem zeigen die Ergebnisse, dass der molekulare Screen die Wirksamkeit des Medikaments überschätzt, da der dropout stärker ist.

Appendix

Score Sheet during therapy

Parameter	**Beobachtung** (Score gilt, wenn eine oder mehrere der genannten Bedingungungen beobachtet wird/werden)	Score
Gewichtsverlust	<5%	0
	≥5% und <10%	1
	≥10% und <15%	3
	≥15% und <20%	5
	≥20%	6
Haltung und Bewegung	normale Bewegung, belastet alle 4 Gliedmaße gleichmäßig	0
	Kauerhaltung, geringgradige Rückenkrümmung, geringgradig verlangsamte Bewegung	1
	mäßige Rückenkrümmung, Kopffehlhaltung, vorsichtiger Gang	3
	ausgeprägte Rückenkrümmung, aufgezogene Bauchdecke, eingezogene Flanken, schwankender/schleppender Gang, deutliche Lahmheit, bewegungsunfähig, Seitenlage	6
Verhalten	aufmerksam, aktiv, neugierig, normale Sozialkontakte	0
	erhöhte Aktivität, eingeschränkte Aktivität	1
	Aggressivität, Stereotypien (z.B. Kreislaufen)	3*
	Apathie, fehlende Reaktion auf äußere Reize	6
Aussehen/Pflege zustand	Fell glatt und glänzend, Haut intakt, sauber und gepflegt	0
	Elefantenzähne, Haarverlust, kahle Stellen, gesträubtes/struppiges Fell	1
	schmutziges/stumpfes Fell, oberflächige Hautläsionen <2cm²	3
	blutige/offene Wunden (> 1 cm²), großflächige Hautläsionen	6
Solider Tumor	nicht tastbar, normales Fell	0
	0 - 1 cm	1
	≥1 - 1,5 cm, Abreibung, Rötung	3
	≥1,5 cm, Ulzeration	6
Augen	offen, sauber, klar	0
	klarer Tränenausfluss, Augen vorübergehend zusammengekniffen	1
	Augen geschlossen/gerötet, eitriger Ausfluss	3
	Auge matt/trüb/eingesunken, Auge und/oder periorbitaler Bereich deutlich geschwollen/blutig, Bulbus tritt vor	6
Atmung	gleichmäßig und regelmäßig	0
	geringgradig erhöhte Atemfrequenz	1
	Atemgeräusche	3
	abdominale Atmung, Maulatmung, Schnappatmung	6

Einzel - Score	Score-Summe	Belastung	Handlungsanweisung	Maßnahmen
0	0	keine	keine spezifische Anweisung	keine
1	2	geringe	Der Projektleiter, seine Vertretung und/oder ein Tierarzt sind hinzuzuziehen	keine
3	3, 4	mittlere	Der Projektleiter, seine Vertretung und/oder ein Tierarzt sind hinzuzuziehen. Ist keine Verbesserung innerhalb von 72 Stunden zu beobachten, wird das Tier tierschutzgerecht getötet	Kontrollfrequenz auf 2x täglich erhöhen. Die Tiere erhalten bei Gewichtsverlust > 10% immer, sonst bei Bedarf: Flüssigkeit (isotonische Kochsalz-lösung), bei Gewichstverlust ≥15% und <20% Gabe von Meloxicam oral 5mg/kg alle 12 bis 24 Stunden.
3*		mittlere	Tiere werden in Einzelkäfige gesetzt und zusätzliches Enrichment zur Verfügung gestellt (rotes Maushäuschen)	
5	5-8	schwere	Der Projektleiter, seine Vertretung und/oder ein Tierarzt sind hinzuzuziehen. Ist keine Verbesserung innerhalb von 72 Stunden zu beobachten, wird das Tier tierschutzgerecht getötet	bei Gewichtsverlust > 10% immer, sonst bei Bedarf: Flüssigkeit (isotonische Kochsalz-lösung), bei Gewichstverlust ≥15% und <20% Gabe von Meloxicam oral 5mg/kg alle 12 bis 24 Stunden.
6	>9	sehr schwere	Tier unverzüglich tierschutzgerecht töten	Projektleiter informieren Und Kadaver zur Organentnahme aufbewahren

Publications

Publications

Christian Augsberger, Gerulf Hänel, Wei Xu, Vesna Pulko, Lydia Jasmin Hanisch, Angelique Augustin, John Challier, **Katharina Hunt**, Binje Vick, Pier Eduardo Rovatti, Christina Krupka, Maurine Rothe, Anne Schönle, Johannes Sam, Emmanuelle Lezan, Axel Ducret, Daniela Ortiz-Franyuti, Antje-Christine Walz, Jörg Benz, Alexander Bujotzek, Felix S Lichtenegger, Christian Gassner, Alejandro Carpy, Victor Lyamichev, Jigar Patel, Nikola P Konstandin, Antje Tunger, Marc Schmitz, Michael von Bergwelt-Baildon, Karsten Spiekermann, Luca Vago, Irmela Jeremias, Estelle Marrer-Berger, Pablo Umaña, Christian Klein, Marion Subklewe. "Targeting intracellular WT1 in AML with a novel RMF-peptide-MHC specific T-cell bispecific antibody". Blood 2021; 138 (25): 2655-2669

Katharina Hunt, Diana Amend, Romina Ludwig, Binje Vick, Anna Katharina Wirth, Tobias Herold, Irmela Jeremias "P323: Streamlining preclinical in vivo treatment trials by multiplexing genetically labelled PDX models of several patients in a single mouse". HemaSphere 6():p 223-224, June 2022

Ehsan Bahrami*, Jan Philipp Schmid*, Vindi Jurinovic, Martin Becker, Anna Katharina Wirth, Romina Ludwig, Sophie Kreissig, Tania Vanessa Duque Angel, Diana Amend, **Katharina Hunt**, Rupert Öllinger, Roland Rad, Jori Maximilian Frenz, Maria Solovey, Frank Ziemann, Matthias Mann, Binje Vick, Christian Wichmann, Tobias Herold, Ashok Kumar Jayavelu, Irmela Jeremias. "Combined proteomics and CRISPR–Cas9 screens in PDX identify ADAM10 as essential for leukemia in vivo". Mol Cancer 2023; 22; 107

Abstracts and Posters

Katharina Hunt, Diana Amend, Romina Ludwig, Binje Vick, Anna Katharina Wirth, Tobias Herold, Irmela Jeremias. Streamlining preclinical in vivo treatment trials by multiplexing genetically labelled PDX models of several patients in a single mouse (P323). EHA2022 Hybrid Congress, Vienna, Austria 2022

Katharina Hunt, Diana Amend, Romina Ludwig, Binje Vick, Anna Katharina Wirth, Tobias Herold, Irmela Jeremias. Streamlining preclinical in vivo treatment trials by multiplexing genetically labelled PDX models in a single mouse. Kind Philipp Meeting 2022

Katharina Hunt, Diana Amend, Romina Ludwig, Binje Vick, Anna Katharina Wirth, Tobias Herold, Irmela Jeremias. Streamlining preclinical in vivo treatment trials by multiplexing genetically labelled PDX models of several patients in a single mouse (EACR22-0210). EACR Congress – Translating biology to medicine, Sevilla, Spain 2022

Bibliography

Adan A, Alizada G, Kiraz Y, Baran Y, Nalbant A. Flow cytometry: basic principles and applications. Crit Rev Biotechnol 2017; 37: 163-76.

Agliano A, Martin-Padura I, Mancuso P, Marighetti P, Rabascio C, Pruneri G, Shultz LD, Bertolini F. Human acute leukemia cells injected in NOD/LtSz-scid/IL-2Rgamma null mice generate a faster and more efficient disease compared to other NOD/scid-related strains. Int J Cancer 2008; 123: 2222-7.

Allen CE, Laetsch TW, Mody R, Irwin MS, Lim MS, Adamson PC, Seibel NL, Parsons DW, Cho YJ, Janeway K, Pediatric MT, Agent Prioritization C. Target and Agent Prioritization for the Children's Oncology Group-National Cancer Institute Pediatric MATCH Trial. J Natl Cancer Inst 2017; 109

Arber DA, Orazi A, Hasserjian R, Thiele J, Borowitz MJ, Le Beau MM, Bloomfield CD, Cazzola M, Vardiman JW. The 2016 revision to the World Health Organization classification of myeloid neoplasms and acute leukemia. Blood 2016; 127: 2391-405.

Ashley EA. Towards precision medicine. Nat Rev Genet 2016; 17: 507-22.

Atherton MJ, Mason NJ. Bite-size introduction to canine hematologic malignancies. Blood Adv 2022; 6: 4073-84.

Avet-loiseau H. Fish Analysis at Diagnosis in Acute Lymphoblastic Leukemia. Leukemia & Lymphoma 1999; 33: 441-9.

Azizian NG, Li Y. XPO1-dependent nuclear export as a target for cancer therapy. J Hematol Oncol 2020; 13: 61.

Bagnyukova TV, Serebriiskii IG, Zhou Y, Hopper-Borge EA, Golemis EA, Astsaturov I. Chemotherapy and signaling: How can targeted therapies supercharge cytotoxic agents? Cancer Biol Ther 2010; 10: 839-53.

Bahrami E, Becker M, Wirth AK, Schmid JP, Herold T, Öllinger R, Rad R, Jeremias I. A CRISPR/Cas9 Library Screen in Patients' Leukemia Cells In Vivo. Blood 2019; 134: 3945.

Bartlett PC, Ruggiero VJ, Hutchinson HC, Droscha CJ, Norby B, Sporer KRB, Taxis TM. Current Developments in the Epidemiology and Control of Enzootic Bovine Leukosis as Caused by Bovine Leukemia Virus. Pathogens 2020; 9: 1058.

Behan FM, Iorio F, Picco G, Gonçalves E, Beaver CM, Migliardi G, Santos R, Rao Y, Sassi F, Pinnelli M, Ansari R, Harper S, Jackson DA, McRae R, Pooley R, Wilkinson P, van der Meer D, Dow D, Buser-Doepner C, Bertotti A, Trusolino L, Stronach EA, Saez-Rodriguez J, Yusa K, Garnett MJ. Prioritization of cancer therapeutic targets using CRISPR-Cas9 screens. Nature 2019; 568: 511-6.

Bennett AL, Williams LE, Ferguson MW, Hauck ML, Suter SE, Lanier CB, Hess PR. Canine acute leukaemia: 50 cases (1989-2014). Vet Comp Oncol 2017; 15: 1101-14.

Bertotti A, Migliardi G, Galimi F, Sassi F, Torti D, Isella C, Cora D, Di Nicolantonio F, Buscarino M, Petti C, Ribero D, Russolillo N, Muratore A, Massucco P, Pisacane A, Molinaro L, Valtorta E, Sartore-Bianchi A, Risio M, Capussotti L, Gambacorta M, Siena S, Medico E, Sapino A, Marsoni S, Comoglio PM, Bardelli A, Trusolino L. A molecularly annotated platform of patient-derived xenografts ("xenopatients") identifies HER2 as an effective therapeutic target in cetuximab-resistant colorectal cancer. Cancer Discov 2011; 1: 508-23.

Bonnet D, Dick JE. Human acute myeloid leukemia is organized as a hierarchy that originates from a primitive hematopoietic cell. Nat Med 1997; 3: 730-7.

Borgmann A, Baldy C, Stackelberg AV, Beyermann B, Fichtner I, Nürnberg P, Henze G. CHILDHOOD ALL BLASTS RETAIN PHENOTYPIC AND GENOTYPIC CHARACTERISTICS UPON LONG-TERM SERIAL PASSAGE IN NOD/SCID MICE. Pediatric Hematology and Oncology 2000; 17: 635-50.

Bose P, Vachhani P, Cortes JE. Treatment of Relapsed/Refractory Acute Myeloid Leukemia. Curr Treat Options Oncol 2017; 18: 17.

Bramlett C, Jiang D, Nogalska A, Eerdeng J, Contreras J, Lu R. Clonal tracking using embedded viral barcoding and high-throughput sequencing. Nat Protoc 2020; 15: 1436-58.

Brinster RL, Chen HY, Warren R, Sarthy A, Palmiter RD. Regulation of metallothionein--thymidine kinase fusion plasmids injected into mouse eggs. Nature 1982; 296: 39-42.

Brown P, Inaba H, Annesley C, Beck J, Colace S, Dallas M, DeSantes K, Kelly K, Kitko C, Lacayo N, Larrier N, Maese L, Mahadeo K, Nanda R, Nardi V, Rodriguez V, Rossoff J, Schuettpelz L, Silverman L, Sun J, Sun W, Teachey D, Wong V, Yanik G, Johnson-Chilla A, Ogba N. Pediatric Acute Lymphoblastic Leukemia, Version 2.2020, NCCN Clinical Practice Guidelines in Oncology. J Natl Compr Canc Netw 2020; 18: 81-112.

Brugman MH, Wiekmeijer AS, van Eggermond M, Wolvers-Tettero I, Langerak AW, de Haas EF, Bystrykh LV, van Rood JJ, de Haan G, Fibbe WE, Staal FJ. Development of a diverse human T-cell repertoire despite stringent restriction of hematopoietic clonality in the thymus. Proc Natl Acad Sci U S A 2015; 112: E6020-7.

Burd A, Levine RL, Ruppert AS, Mims AS, Borate U, Stein EM, Patel P, Baer MR, Stock W, Deininger M, Blum W, Schiller G, Olin R, Litzow M, Foran J, Lin TL, Ball B, Boyiadzis M, Traer E, Odenike O, Arellano M, Walker A, Duong VH, Kovacsovics T, Collins R, Shoben AB, Heerema NA, Foster MC, Vergilio JA, Brennan T, Vietz C, Severson E, Miller M, Rosenberg L, Marcus S, Yocum A, Chen T, Stefanos M, Druker B, Byrd JC. Precision medicine treatment in acute myeloid leukemia using prospective genomic profiling: feasibility and preliminary efficacy of the Beat AML Master Trial. Nat Med 2020; 26: 1852-8.

Camus V, Miloudi H, Taly A, Sola B, Jardin F. XPO1 in B cell hematological malignancies: from recurrent somatic mutations to targeted therapy. J Hematol Oncol 2017; 10: 47.

Carlet M, Völse K, Vergalli J, Becker M, Herold T, Arner A, Senft D, Jurinovic V, Liu WH, Gao Y, Dill V, Fehse B, Baldus CD, Bastian L, Lenk L, Schewe DM, Bagnoli JW, Vick B, Schmid JP, Wilhelm A, Marschalek R, Jost PJ, Miething C, Riecken K, Schmidt-Supprian M, Binder V, Jeremias I. In vivo inducible reverse genetics in patients' tumors to identify individual therapeutic targets. Nat Commun 2021; 12: 5655.

Castro Alves C, Terziyska N, Grunert M, Gundisch S, Graubner U, Quintanilla-Martinez L, Jeremias I. Leukemia-initiating cells of patient-derived acute lymphoblastic leukemia xenografts are sensitive toward TRAIL. Blood 2012; 119: 4224-7.

Cesano A, Hoxie JA, Lange B, Nowell PC, Bishop J, Santoli D. The severe combined immunodeficient (SCID) mouse as a model for human myeloid leukemias. Oncogene 1992; 7: 827-36.

Cheon DJ, Orsulic S. Mouse models of cancer. Annu Rev Pathol 2011; 6: 95-119.

Cho SY. Patient-derived xenografts as compatible models for precision oncology. Lab Anim Res 2020; 36: 14.

Cornell RF, Baz R, Richter JR, Rossi A, Vogl DT, Chen C, Shustik C, Alvarez MJ, Shen Y, Unger TJ, Ben-Shahar O, Wang H, Baloglu E, Senapedis W, Ma X, Landesman Y, Bai X, Bader J, Xu H, Marshall T, Chang H, Walker CJ, Shah J, Shacham S, Kauffman MG, Hofmeister CC. A phase 1 clinical trial of oral eltanexor in patients with relapsed or refractory multiple myeloma. Am J Hematol 2022; 97: E54-E8.

Cornils K, Thielecke L, Huser S, Forgber M, Thomaschewski M, Kleist N, Hussein K, Riecken K, Volz T, Gerdes S, Glauche I, Dahl A, Dandri M, Roeder I, Fehse B. Multiplexing clonality: combining RGB marking and genetic barcoding. Nucleic Acids Res 2014; 42: e56.

Coustan-Smith E, Kitanaka A, Pui CH, McNinch L, Evans WE, Raimondi SC, Behm FG, Arico M, Campana D. Clinical relevance of BCL-2 overexpression in childhood acute lymphoblastic leukemia. Blood 1996; 87: 1140-6.

Coyne GO, Takebe N, Chen AP. Defining precision: The precision medicine initiative trials NCI-MPACT and NCI-MATCH. Curr Probl Cancer 2017; 41: 182-93.

Cuppen E, Elemento O, Rosenquist R, Nikic S, M IJ, Zaleski ID, Frederix G, Levin LA, Mullighan CG, Buettner R, Pugh TJ, Grimmond S, Caldas C, Andre F, Custers I, Campo E, van Snellenberg H, Schuh A, Nakagawa H, von Kalle C, Haferlach T, Frohling S, Jobanputra V. Implementation of Whole-Genome and Transcriptome Sequencing Into Clinical Cancer Care. JCO Precis Oncol 2022; 6: e2200245.

Dempster JM, Pacini C, Pantel S, Behan FM, Green T, Krill-Burger J, Beaver CM, Younger ST, Zhivich V, Najgebauer H, Allen F, Goncalves E, Shepherd R, Doench JG, Yusa K, Vazquez F, Parts L, Boehm JS, Golub TR, Hahn WC, Root DE, Garnett MJ, Tsherniak A, Iorio F. Agreement between two large pan-cancer CRISPR-Cas9 gene dependency data sets. Nat Commun 2019; 10: 5817.

Deng J, Carlson N, Takeyama K, Dal Cin P, Shipp M, Letai A. BH3 profiling identifies three distinct classes of apoptotic blocks to predict response to ABT-737 and conventional chemotherapeutic agents. Cancer Cell 2007; 12: 171-85.

Dohner H, Estey E, Grimwade D, Amadori S, Appelbaum FR, Buchner T, Dombret H, Ebert BL, Fenaux P, Larson RA, Levine RL, Lo-Coco F, Naoe T, Niederwieser D, Ossenkoppele GJ, Sanz M, Sierra J, Tallman MS, Tien HF, Wei AH, Lowenberg B, Bloomfield CD. Diagnosis and management of AML in adults: 2017 ELN recommendations from an international expert panel. Blood 2017; 129: 424-47.
Döhner H, Wei AH, Löwenberg B. Towards precision medicine for AML. Nat Rev Clin Oncol 2021; 18: 577-90.

Dong Y, Shi O, Zeng Q, Lu X, Wang W, Li Y, Wang Q. Leukemia incidence trends at the global, regional, and national level between 1990 and 2017. Exp Hematol Oncol 2020; 9: 14.

Doudna JA, Charpentier E. Genome editing. The new frontier of genome engineering with CRISPR-Cas9. Science 2014; 346: 1258096.

Ebinger S, Ozdemir EZ, Ziegenhain C, Tiedt S, Castro Alves C, Grunert M, Dworzak M, Lutz C, Turati VA, Enver T, Horny HP, Sotlar K, Parekh S, Spiekermann K, Hiddemann W, Schepers A, Polzer B, Kirsch S, Hoffmann M, Knapp B, Hasenauer J, Pfeifer H, Panzer-Grumayer R, Enard W, Gires O, Jeremias I. Characterization of Rare, Dormant, and Therapy-Resistant Cells in Acute Lymphoblastic Leukemia. Cancer Cell 2016; 30: 849-62.

Elder A, Bomken S, Wilson I, Blair HJ, Cockell S, Ponthan F, Dormon K, Pal D, Heidenreich O, Vormoor J. Abundant and equipotent founder cells establish and maintain acute lymphoblastic leukaemia. Leukemia 2017; 31: 2577-86.

Epperly E, Hume KR, Moirano S, Stokol T, Intile J, Erb HN, Scrivani PV. Dogs with acute myeloid leukemia or lymphoid neoplasms (large cell lymphoma or acute lymphoblastic leukemia) may have indistinguishable mediastinal masses on radiographs. Vet Radiol Ultrasound 2018; 59: 507-15.

Etchin J, Berezovskaya A, Conway AS, Galinsky IA, Stone RM, Baloglu E, Senapedis W, Landesman Y, Kauffman M, Shacham S, Wang JC, Look AT. KPT-8602, a second-generation inhibitor of XPO1-mediated nuclear export, is well tolerated and highly active against AML blasts and leukemia-initiating cells. Leukemia 2017; 31: 143-50.

Forrest SJ, Geoerger B, Janeway KA. Precision medicine in pediatric oncology. Curr Opin Pediatr 2018; 30: 17-24.

Gao H, Korn JM, Ferretti S, Monahan JE, Wang Y, Singh M, Zhang C, Schnell C, Yang G, Zhang Y, Balbin OA, Barbe S, Cai H, Casey F, Chatterjee S, Chiang DY, Chuai S, Cogan SM, Collins SD, Dammassa E, Ebel N, Embry M, Green J, Kauffmann A, Kowal C, Leary RJ, Lehar J, Liang Y, Loo A, Lorenzana E, Robert McDonald E, 3rd, McLaughlin ME, Merkin J, Meyer R, Naylor TL, Patawaran M, Reddy A, Roelli C, Ruddy DA, Salangsang F, Santacroce F, Singh AP, Tang Y, Tinetto W, Tobler S, Velazquez R, Venkatesan K, Von Arx F, Wang HQ, Wang Z, Wiesmann M, Wyss D, Xu F, Bitter H, Atadja P, Lees E, Hofmann F, Li E, Keen N, Cozens R, Jensen MR, Pryer NK, Williams JA, Sellers WR. High-throughput screening using patient-derived tumor xenografts to predict clinical trial drug response. Nat Med 2015; 21: 1318-25.

Ghalandary M, Gao Y, Amend D, Kutkaite G, Vick B, Spiekermann K, Rothenberg-Thurley M, Metzeler KH, Marcinek A, Subklewe M, Menden MP, Jurinovic V, Bahrami E, Jeremias I. WT1 and DNMT3A play essential roles in the growth of certain patient AML cells in mice. Blood 2022; 141: 955-960.

Gonçalves E, Segura-Cabrera A, Pacini C, Picco G, Behan FM, Jaaks P, Coker EA, van der Meer D, Barthorpe A, Lightfoot H, Mironenko T, Beck A, Richardson L, Yang W, Lleshi E, Hall J, Tolley C, Hall C, Mali I, Thomas F, Morris J, Leach AR, Lynch JT, Sidders B, Crafter C, Iorio F, Fawell S, Garnett MJ. Drug mechanism-of-action discovery through the integration of pharmacological and CRISPR screens. Mol Syst Biol 2020; 16: e9405.
Gores GJ, Kaufmann SH. Selectively targeting Mcl-1 for the treatment of acute myelogenous leukemia and solid tumors. Genes Dev 2012; 26: 305-11.

Govaerts I, Prieto C, Vandersmissen C, Gielen O, Jacobs K, Provost S, Nittner D, Maertens J, Boeckx N, De Keersmaecker K, Segers H, Cools J. PSEN1-selective gamma-secretase inhibition in combination with kinase or XPO-1 inhibitors effectively targets T cell acute lymphoblastic leukemia. J Hematol Oncol 2021; 14: 97.

Harrison DE. Competitive repopulation: a new assay for long-term stem cell functional capacity. Blood 1980; 55: 77-81.

Hassold T, Hunt P. To err (meiotically) is human: the genesis of human aneuploidy. Nat Rev Genet 2001; 2: 280-91.

Heuser M, Smith BD, Fiedler W, Sekeres MA, Montesinos P, Leber B, Merchant A, Papayannidis C, Perez-Simon JA, Hoang CJ, O'Brien T, Ma WW, Zeremski M, O'Connell A, Chan G, Cortes JE. Clinical benefit of glasdegib plus low-dose cytarabine in patients with de novo and secondary acute myeloid leukemia: long-term analysis of a phase II randomized trial. Ann Hematol 2021; 100: 1181-94.

Hidalgo M, Amant F, Biankin AV, Budinska E, Byrne AT, Caldas C, Clarke RB, de Jong S, Jonkers J, Maelandsmo GM, Roman-Roman S, Seoane J, Trusolino L, Villanueva A. Patient-derived xenograft models: an emerging platform for translational cancer research. Cancer Discov 2014; 4: 998-1013.

Hofmann-Lehmann R, Hartmann K. Feline leukaemia virus infection: A practical approach to diagnosis. J Feline Med Surg 2020; 22: 831-46.

Houshmand M, Blanco TM, Circosta P, Yazdi N, Kazemi A, Saglio G, Zarif MN. Bone marrow microenvironment: The guardian of leukemia stem cells. World J Stem Cells 2019; 11: 476-90.

Hunger SP, Raetz EA. How I treat relapsed acute lymphoblastic leukemia in the pediatric population. Blood 2020; 136: 1803-12.

Hunt K, Amend D, Ludwig R, Vick B, Wirth AK, Herold T, Jeremias I. Streamlining preclinical in vivo treatment trials by multiplexing genetically labelled PDX models of several patients in a single mouse Hemasphere 2022; 6: 223-224.

Inaba H, Mullighan CG. Pediatric acute lymphoblastic leukemia. Haematologica 2020; 105: 2524-39.

Jiang J, Yuan J, Hu Z, Zhang Y, Zhang T, Xu M, Long M, Fan Y, Tanyi JL, Montone KT, Tavana O, Vonderheide RH, Chan HM, Hu X, Zhang L. Systematic illumination of druggable genes in cancer genomes. Cell Rep 2022; 38: 110400.

Kamel-Reid S, Letarte M, Sirard C, Doedens M, Grunberger T, Fulop G, Freedman MH, Phillips RA, Dick JE. A model of human acute lymphoblastic leukemia in immune-deficient SCID mice. Science 1989; 246: 1597-600.

Kim-Wanner S-Z, Kraywinkel K. Faktenblatt: Epidemiologie der akuten Leukämien in Deutschland 2016 bis 2018. Die Onkologie 2022; 28: 459-62.
Koss B, Morrison J, Perciavalle RM, Singh H, Rehg JE, Williams RT, Opferman JT. Requirement for antiapoptotic MCL-1 in the survival of BCR-ABL B-lineage acute lymphoblastic leukemia. Blood 2013; 122: 1587-98.

Kotschy A, Szlavik Z, Murray J, Davidson J, Maragno AL, Le Toumelin-Braizat G, Chanrion M, Kelly GL, Gong JN, Moujalled DM, Bruno A, Csekei M, Paczal A, Szabo ZB, Sipos S, Radics G, Proszenyak A, Balint B, Ondi L, Blasko G, Robertson A, Surgenor A, Dokurno P, Chen I, Matassova N, Smith J, Pedder C, Graham C, Studeny A, Lysiak-Auvity G, Girard AM, Grave F, Segal D, Riffkin CD, Pomilio G, Galbraith LC, Aubrey BJ, Brennan MS, Herold MJ, Chang C, Guasconi G, Cauquil N, Melchiore F, Guigal-Stephan N, Lockhart B, Colland F, Hickman JA, Roberts AW, Huang DC, Wei AH, Strasser A, Lessene G, Geneste O. The MCL1 inhibitor S63845 is tolerable and effective in diverse cancer models. Nature 2016; 538: 477-82.

Kuwata T, Yanagihara K, Iino Y, Komatsu T, Ochiai A, Sekine S, Taniguchi H, Katai H, Kinoshita T, Ohtsu A. Establishment of Novel Gastric Cancer Patient-Derived Xenografts and Cell Lines: Pathological Comparison between Primary Tumor, Patient-Derived, and Cell-Line Derived Xenografts. Cells 2019; 8

Kwarteng EO, Heinonen KM. Competitive Transplants to Evaluate Hematopoietic Stem Cell Fitness. J Vis Exp 2016; 114: 54345.

Lassen UN, Makaroff LE, Stenzinger A, Italiano A, Vassal G, Garcia-Foncillas J, Avouac B. Precision oncology: a clinical and patient perspective. Future Oncol 2021; 17: 3995-4009.

Lau LMS, Mayoh C, Xie J, Barahona P, MacKenzie KL, Wong M, Kamili A, Tsoli M, Failes TW, Kumar A, Mould EVA, Gifford A, Chow SO, Pinese M, Fletcher JI, Arndt GM, Khuong-Quang DA,

Wadham C, Batey D, Eden G, Trebilcock P, Joshi S, Alfred S, Gopalakrishnan A, Khan A, Grebert Wade D, Strong PA, Manouvrier E, Morgan LT, Span M, Lim JY, Cadiz R, Ung C, Thomas DM, Tucker KM, Warby M, McCowage GB, Dalla-Pozza L, Byrne JA, Saletta F, Fellowes A, Fox SB, Norris MD, Tyrrell V, Trahair TN, Lock RB, Cowley MJ, Ekert PG, Haber M, Ziegler DS, Marshall GM. In vitro and in vivo drug screens of tumor cells identify novel therapies for high-risk child cancer. EMBO Mol Med 2022; 14: e14608.

Lawrence MS, Stojanov P, Mermel CH, Robinson JT, Garraway LA, Golub TR, Meyerson M, Gabriel SB, Lander ES, Getz G. Discovery and saturation analysis of cancer genes across 21 tumour types. Nature 2014; 505: 495-501.

le Viseur C, Hotfilder M, Bomken S, Wilson K, Rottgers S, Schrauder A, Rosemann A, Irving J, Stam RW, Shultz LD, Harbott J, Jurgens H, Schrappe M, Pieters R, Vormoor J. In childhood acute lymphoblastic leukemia, blasts at different stages of immunophenotypic maturation have stem cell properties. Cancer Cell 2008; 14: 47-58.

Lee S, Mohan S, Knupp J, Chamoun K, Bai X, Ma X, Shah JJ, Kauffman M, Shacham S, Bhatnagar B. Updated overall survival of eltanexor for the treatment of patients with hypomethylating agent refractory myelodysplastic syndrome. Journal of Clinical Oncology 2021; 39: e19037-e.

Lee S, Mohan S, Knupp J, Chamoun K, de Jonge A, Yang F, Baloglu E, Shah J, Kauffman MG, Shacham S, Bhatnagar B. Oral eltanexor treatment of patients with higher-risk myelodysplastic syndrome refractory to hypomethylating agents. J Hematol Oncol 2022; 15: 103.
Li Z, He S, Look AT. The MCL1-specific inhibitor S63845 acts synergistically with venetoclax/ABT-199 to induce apoptosis in T-cell acute lymphoblastic leukemia cells. Leukemia 2019; 33: 262-6.

Li Z, Zheng W, Wang H, Cheng Y, Fang Y, Wu F, Sun G, Sun G, Lv C, Hui B. Application of Animal Models in Cancer Research: Recent Progress and Future Prospects. Cancer Manag Res 2021; 13: 2455-75.

Liao D. Emerging roles of the EBF family of transcription factors in tumor suppression. Mol Cancer Res 2009; 7: 1893-901.

Liem NL, Papa RA, Milross CG, Schmid MA, Tajbakhsh M, Choi S, Ramirez CD, Rice AM, Haber M, Norris MD, MacKenzie KL, Lock RB. Characterization of childhood acute lymphoblastic leukemia xenograft models for the preclinical evaluation of new therapies. Blood 2004; 103: 3905-14.

Little S, Levy J, Hartmann K, Hofmann-Lehmann R, Hosie M, Olah G, Denis KS. 2020 AAFP Feline Retrovirus Testing and Management Guidelines. J Feline Med Surg 2020; 22: 5-30.

Liu WH, Mrozek-Gorska P, Wirth AK, Herold T, Schwarzkopf L, Pich D, Volse K, Melo-Narvaez MC, Carlet M, Hammerschmidt W, Jeremias I. Inducible transgene expression in PDX models in vivo identifies KLF4 as a therapeutic target for B-ALL. Biomark Res 2020; 8: 46.

Lock RB, Liem N, Farnsworth ML, Milross CG, Xue C, Tajbakhsh M, Haber M, Norris MD, Marshall GM, Rice AM. The nonobese diabetic/severe combined immunodeficient (NOD/SCID) mouse model of childhood acute lymphoblastic leukemia reveals intrinsic differences in biologic characteristics at diagnosis and relapse. Blood 2002; 99: 4100-8.

Maetzig T, Ruschmann J, Sanchez Milde L, Lai CK, von Krosigk N, Humphries RK. Lentiviral Fluorescent Genetic Barcoding for Multiplex Fate Tracking of Leukemic Cells. Mol Ther Methods Clin Dev 2017; 6: 54-65.

Maetzig T, Morgan M, Schambach A. Fluorescent genetic barcoding for cellular multiplex analyses. Exp Hematol 2018; 67: 10-7.

Maezawa M, Akiyama N, Tagawa M, Watanabe KI, Matsumoto K, Furuoka H, Inokuma H. A clinical case of acute myelomonocytic leukemia in a Holstein cow. J Vet Med Sci 2021; 83: 819-23.

Mak IW, Evaniew N, Ghert M. Lost in translation: animal models and clinical trials in cancer treatment. Am J Transl Res 2014; 6: 114-8.

Malani D, Kumar A, Bruck O, Kontro M, Yadav B, Hellesoy M, Kuusanmaki H, Dufva O, Kankainen M, Eldfors S, Potdar S, Saarela J, Turunen L, Parsons A, Vastrik I, Kivinen K, Saarela J, Raty R, Lehto M, Wolf M, Gjertsen BT, Mustjoki S, Aittokallio T, Wennerberg K, Heckman CA, Kallioniemi O, Porkka K. Implementing a Functional Precision Medicine Tumor Board for Acute Myeloid Leukemia. Cancer Discov 2022; 12: 388-401.

Manzano-Munoz A, Yeste J, Ortega MA, Martin F, Lopez A, Rosell J, Castro S, Serrano C, Samitier J, Ramon-Azcon J, Montero J. Microfluidic-based dynamic BH3 profiling predicts anticancer treatment efficacy. NPJ Precis Oncol 2022; 6: 90.
Marcotte R, Sayad A, Brown KR, Sanchez-Garcia F, Reimand J, Haider M, Virtanen C, Bradner JE, Bader GD, Mills GB, Pe'er D, Moffat J, Neel BG. Functional Genomic Landscape of Human Breast Cancer Drivers, Vulnerabilities, and Resistance. Cell 2016; 164: 293-309.

Marquart J, Chen EY, Prasad V. Estimation of the Percentage of US Patients With Cancer Who Benefit From Genome-Driven Oncology. JAMA Oncol 2018; 4: 1093-8.

Meijer TG, Naipal KA, Jager A, van Gent DC. Ex vivo tumor culture systems for functional drug testing and therapy response prediction. Future Sci OA 2017; 3: FSO190.

Meyer LH, Debatin KM. Diversity of human leukemia xenograft mouse models: implications for disease biology. Cancer Res 2011; 71: 7141-4.

Mitra A, Mishra L, Li S. Technologies for deriving primary tumor cells for use in personalized cancer therapy. Trends Biotechnol 2013; 31: 347-54.

Moujalled DM, Hanna DT, Hediyeh-Zadeh S, Pomilio G, Brown L, Litalien V, Bartolo R, Fleming S, Chanrion M, Banquet S, Maragno AL, Kraus-Berthier L, Schoumacher M, Mullighan CG, Georgiou A, White CA, Lessene G, Huang DCS, Roberts AW, Geneste O, Rasmussen L, Davis MJ, Ekert PG, Wei A, Ng AP, Khaw SL. Cotargeting BCL-2 and MCL-1 in high-risk B-ALL. Blood Adv 2020; 4: 2762-7.

Mullighan CG, Goorha S, Radtke I, Miller CB, Coustan-Smith E, Dalton JD, Girtman K, Mathew S, Ma J, Pounds SB, Su X, Pui CH, Relling MV, Evans WE, Shurtleff SA, Downing JR. Genome-wide analysis of genetic alterations in acute lymphoblastic leukaemia. Nature 2007; 446: 758-64.

Mullighan CG, Phillips LA, Su X, Ma J, Miller CB, Shurtleff SA, Downing JR. Genomic analysis of the clonal origins of relapsed acute lymphoblastic leukemia. Science 2008; 322: 1377-80.

Nijmeijer BA, Mollevanger P, van Zelderen-Bhola SL, Kluin-Nelemans HC, Willemze R, Falkenburg JH. Monitoring of engraftment and progression of acute lymphoblastic leukemia in individual NOD/SCID mice. Exp Hematol 2001; 29: 322-9.

Nutt SL, Heavey B, Rolink AG, Busslinger M. Commitment to the B-lymphoid lineage depends on the transcription factor Pax5. Nature 1999; 401: 556-62.

Pan C, Kumar C, Bohl S, Klingmueller U, Mann M. Comparative proteomic phenotyping of cell lines and primary cells to assess preservation of cell type-specific functions. Mol Cell Proteomics 2009; 8: 443-50.

Pan R, Hogdal LJ, Benito JM, Bucci D, Han L, Borthakur G, Cortes J, DeAngelo DJ, Debose L, Mu H, Dohner H, Gaidzik VI, Galinsky I, Golfman LS, Haferlach T, Harutyunyan KG, Hu J, Leverson JD, Marcucci G, Muschen M, Newman R, Park E, Ruvolo PP, Ruvolo V, Ryan J, Schindela S, Zweidler-McKay P, Stone RM, Kantarjian H, Andreeff M, Konopleva M, Letai AG. Selective BCL-2 inhibition by ABT-199 causes on-target cell death in acute myeloid leukemia. Cancer Discov 2014; 4: 362-75.

Pemovska T, Kontro M, Yadav B, Edgren H, Eldfors S, Szwajda A, Almusa H, Bespalov MM, Ellonen P, Elonen E, Gjertsen BT, Karjalainen R, Kulesskiy E, Lagstrom S, Lehto A, Lepisto M, Lundan T, Majumder MM, Marti JM, Mattila P, Murumagi A, Mustjoki S, Palva A, Parsons A, Pirttinen T, Ramet ME, Suvela M, Turunen L, Vastrik I, Wolf M, Knowles J, Aittokallio T, Heckman CA, Porkka K, Kallioniemi O, Wennerberg K. Individualized systems medicine strategy to tailor treatments for patients with chemorefractory acute myeloid leukemia. Cancer Discov 2013; 3: 1416-29.

Pompili L, Porru M, Caruso C, Biroccio A, Leonetti C. Patient-derived xenografts: a relevant preclinical model for drug development. J Exp Clin Cancer Res 2016; 35: 189.

Potter DS, Du R, Bhola P, Bueno R, Letai A. Dynamic BH3 profiling identifies active BH3 mimetic combinations in non-small cell lung cancer. Cell Death Dis 2021; 12: 741.

Prasad V. Perspective: The precision-oncology illusion. Nature 2016; 537: S63.

Richmond A, Su Y. Mouse xenograft models vs GEM models for human cancer therapeutics. Dis Model Mech 2008; 1: 78-82.

Roberts AW, Wei AH, Huang DCS. BCL2 and MCL1 inhibitors for hematologic malignancies. Blood 2021; 138: 1120-36.

Robertson LE, Plunkett W, McConnell K, Keating MJ, McDonnell TJ. Bcl-2 expression in chronic lymphocytic leukemia and its correlation with the induction of apoptosis and clinical outcome. Leukemia 1996; 10: 456-9.

Roife D, Dai B, Kang Y, Perez MVR, Pratt M, Li X, Fleming JB. Ex Vivo Testing of Patient-Derived Xenografts Mirrors the Clinical Outcome of Patients with Pancreatic Ductal Adenocarcinoma. Clin Cancer Res 2016; 22: 6021-30.

Roskoski R, Jr. Properties of FDA-approved small molecule protein kinase inhibitors: A 2021 update. Pharmacol Res 2021; 165: 105463.

Rosler ES, Brandt JE, Chute J, Hoffman R. An in vivo competitive repopulation assay for various sources of human hematopoietic stem cells. Blood 2000; 96: 3414-21.

Ross JS, Schenkein DP, Pietrusko R, Rolfe M, Linette GP, Stec J, Stagliano NE, Ginsburg GS, Symmans WF, Pusztai L, Hortobagyi GN. Targeted therapies for cancer 2004. Am J Clin Pathol 2004; 122: 598-609.

Russell WMS, Burch RL (1959) The principles of humane experimental technique. Methuen

Rygaard J, Povlsen CO. Heterotransplantation of a human malignant tumour to "Nude" mice. Acta Pathol Microbiol Scand 1969; 77: 758-60.

Sajjad H, Imtiaz S, Noor T, Siddiqui YH, Sajjad A, Zia M. Cancer models in preclinical research: A chronicle review of advancement in effective cancer research. Animal Model Exp Med 2021; 4: 87-103.

Salah HT, DiNardo CD, Konopleva M, Khoury JD. Potential Biomarkers for Treatment Response to the BCL-2 Inhibitor Venetoclax: State of the Art and Future Directions. Cancers (Basel) 2021; 13

Salvaris R, Fedele PL. Targeted Therapy in Acute Lymphoblastic Leukaemia. J Pers Med 2021; 11 (8): 715.

Sawyers C. Targeted cancer therapy. Nature 2004; 432: 294-7.

Schmitz M, Breithaupt P, Scheidegger N, Cario G, Bonapace L, Meissner B, Mirkowska P, Tchinda J, Niggli FK, Stanulla M, Schrappe M, Schrauder A, Bornhauser BC, Bourquin JP. Xenografts of highly resistant leukemia recapitulate the clonal composition of the leukemogenic compartment. Blood 2011; 118: 1854-64.

Schueler J, Klingner K, Bug D, Zoeller C, Maier A, Dong M, Willecke K, Peille AL, Steiner E, Landesfeind M, Copland JA, Siegers GM, Haferkamp A, Boehm K, Tsaur I, Schneider M. Patient derived renal cell carcinoma xenografts exhibit distinct sensitivity patterns in response to antiangiogenic therapy and constitute a suitable tool for biomarker development. Oncotarget 2018; 9: 30946-61.

Seyfried F, Demir S, Horl RL, Stirnweiss FU, Ryan J, Scheffold A, Villalobos-Ortiz M, Boldrin E, Zinngrebe J, Enzenmuller S, Jenni S, Tsai YC, Bornhauser B, Furstberger A, Kraus JM, Kestler HA, Bourquin JP, Stilgenbauer S, Letai A, Debatin KM, Meyer LH. Prediction of venetoclax activity in precursor B-ALL by functional assessment of apoptosis signaling. Cell Death Dis 2019; 10: 571.

Seyfried F, Stirnweiss FU, Niedermayer A, Enzenmuller S, Horl RL, Munch V, Kohrer S, Debatin KM, Meyer LH. Synergistic activity of combined inhibition of anti-apoptotic molecules in B-cell precursor ALL. Leukemia 2022; 36: 901-12.

Shalem O, Sanjana NE, Hartenian E, Shi X, Scott DA, Mikkelson T, Heckl D, Ebert BL, Root DE, Doench JG, Zhang F. Genome-scale CRISPR-Cas9 knockout screening in human cells. Science 2014; 343: 84-7.

Short NJ, Konopleva M, Kadia TM, Borthakur G, Ravandi F, DiNardo CD, Daver N. Advances in the Treatment of Acute Myeloid Leukemia: New Drugs and New Challenges. Cancer Discov 2020; 10: 506-25.

Shultz LD, Lyons BL, Burzenski LM, Gott B, Chen X, Chaleff S, Kotb M, Gillies SD, King M, Mangada J, Greiner DL, Handgretinger R. Human lymphoid and myeloid cell development in NOD/LtSz-scid IL2R gamma null mice engrafted with mobilized human hemopoietic stem cells. J Immunol 2005; 174: 6477-89.

Siegel RL, Miller KD, Fuchs HE, Jemal A. Cancer statistics, 2022. CA Cancer J Clin 2022; 72: 7-33.

Siolas D, Hannon GJ. Patient-derived tumor xenografts: transforming clinical samples into mouse models. Cancer Res 2013; 73: 5315-9.

Souers AJ, Leverson JD, Boghaert ER, Ackler SL, Catron ND, Chen J, Dayton BD, Ding H, Enschede SH, Fairbrother WJ, Huang DC, Hymowitz SG, Jin S, Khaw SL, Kovar PJ, Lam LT, Lee J, Maecker HL, Marsh KC, Mason KD, Mitten MJ, Nimmer PM, Oleksijew A, Park CH, Park CM, Phillips DC, Roberts AW, Sampath D, Seymour JF, Smith ML, Sullivan GM, Tahir SK, Tse C, Wendt MD, Xiao Y, Xue JC, Zhang H, Humerickhouse RA, Rosenberg SH, Elmore SW. ABT-199, a potent and selective BCL-2 inhibitor, achieves antitumor activity while sparing platelets. Nat Med 2013; 19: 202-8.

Spinner MA, Aleshin A, Santaguida MT, Schaffert SA, Zehnder JL, Patterson AS, Gekas C, Heiser D, Greenberg PL. Ex vivo drug screening defines novel drug sensitivity patterns for informing personalized therapy in myeloid neoplasms. Blood Adv 2020; 4: 2768-78.

Szilvassy SJ, Humphries RK, Lansdorp PM, Eaves AC, Eaves CJ. Quantitative assay for totipotent reconstituting hematopoietic stem cells by a competitive repopulation strategy. Proc Natl Acad Sci U S A 1990; 87: 8736-40.

Terwilliger T, Abdul-Hay M. Acute lymphoblastic leukemia: a comprehensive review and 2017 update. Blood Cancer J 2017; 7: e577.

Terziyska N, Castro Alves C, Groiss V, Schneider K, Farkasova K, Ogris M, Wagner E, Ehrhardt H, Brentjens RJ, zur Stadt U, Horstmann M, Quintanilla-Martinez L, Jeremias I. In vivo imaging enables high resolution preclinical trials on patients' leukemia cells growing in mice. PLoS One 2012; 7: e52798.

Thol F, Ganser A. Treatment of Relapsed Acute Myeloid Leukemia. Curr Treat Options Oncol 2020; 21: 66.

Tomiyasu H, Doi A, Chambers JK, Goto-Koshino Y, Ohmi A, Ohno K, Tsujimoto H. Clinical and clinicopathological characteristics of acute lymphoblastic leukaemia in six cats. J Small Anim Pract 2018; 59: 742-6.

Townsend EC, Murakami MA, Christodoulou A, Christie AL, Koster J, DeSouza TA, Morgan EA, Kallgren SP, Liu H, Wu SC, Plana O, Montero J, Stevenson KE, Rao P, Vadhi R, Andreeff M, Armand P, Ballen KK, Barzaghi-Rinaudo P, Cahill S, Clark RA, Cooke VG, Davids MS, DeAngelo DJ, Dorfman DM, Eaton H, Ebert BL, Etchin J, Firestone B, Fisher DC, Freedman AS, Galinsky IA, Gao H, Garcia JS, Garnache-Ottou F, Graubert TA, Gutierrez A, Halilovic E, Harris MH, Herbert ZT, Horwitz SM, Inghirami G, Intlekofer AM, Ito M, Izraeli S, Jacobsen ED, Jacobson CA, Jeay S, Jeremias I, Kelliher MA, Koch R, Konopleva M, Kopp N, Kornblau SM, Kung AL, Kupper TS, LeBoeuf NR, LaCasce AS, Lees E, Li LS, Look AT, Murakami M, Muschen M, Neuberg D, Ng SY, Odejide OO, Orkin SH, Paquette RR, Place AE, Roderick JE, Ryan JA, Sallan SE, Shoji B, Silverman LB, Soiffer RJ, Steensma DP, Stegmaier K, Stone RM, Tamburini J, Thorner AR, van Hummelen P, Wadleigh M, Wiesmann M, Weng AP, Wuerthner JU, Williams DA, Wollison BM, Lane AA, Letai A, Bertagnolli MM, Ritz J, Brown M, Long H, Aster JC, Shipp MA, Griffin JD, Weinstock DM. The Public Repository of Xenografts Enables Discovery and Randomized Phase II-like Trials in Mice. Cancer Cell 2016; 30: 183.

Tyner JW, Tognon CE, Bottomly D, Wilmot B, Kurtz SE, Savage SL, Long N, Schultz AR, Traer E, Abel M, Agarwal A, Blucher A, Borate U, Bryant J, Burke R, Carlos A, Carpenter R, Carroll J, Chang BH, Coblentz C, d'Almeida A, Cook R, Danilov A, Dao KT, Degnin M, Devine D, Dibb J, Edwards DKt, Eide CA, English I, Glover J, Henson R, Ho H, Jemal A, Johnson K, Johnson R, Junio B, Kaempf A, Leonard J, Lin C, Liu SQ, Lo P, Loriaux MM, Luty S, Macey T, MacManiman J, Martinez J, Mori M, Nelson D, Nichols C, Peters J, Ramsdill J, Rofelty A, Schuff R, Searles R, Segerdell E, Smith RL, Spurgeon SE, Sweeney T, Thapa A, Visser C, Wagner J, Watanabe-Smith K, Werth K, Wolf J, White L, Yates A, Zhang H, Cogle CR, Collins RH, Connolly DC, Deininger MW, Drusbosky L, Hourigan CS, Jordan CT, Kropf P, Lin TL, Martinez ME, Medeiros BC, Pallapati RR, Pollyea DA, Swords RT, Watts JM, Weir SJ, Wiest DL, Winters RM, McWeeney SK, Druker BJ. Functional genomic landscape of acute myeloid leukaemia. Nature 2018; 562: 526-31.

Valtieri M, Schiro R, Chelucci C, Masella B, Testa U, Casella I, Montesoro E, Mariani G, Hassan HJ, Peschle C. Efficient transfer of selectable and membrane reporter genes in hematopoietic progenitor and stem cells purified from human peripheral blood. Cancer Res 1994; 54: 4398-404.

van Tilburg CM, Pfaff E, Pajtler KW, Langenberg KPS, Fiesel P, Jones BC, Balasubramanian GP, Stark S, Johann PD, Blattner-Johnson M, Schramm K, Dikow N, Hirsch S, Sutter C, Grund K, von Stackelberg A, Kulozik AE, Lissat A, Borkhardt A, Meisel R, Reinhardt D, Klusmann JH, Fleischhack G, Tippelt S, von Schweinitz D, Schmid I, Kramm CM, von Bueren AO, Calaminus G, Vorwerk P, Graf N, Westermann F, Fischer M, Eggert A, Burkhardt B, Wossmann W, Nathrath M, Hecker-Nolting S, Fruhwald MC, Schneider DT, Brecht IB, Ketteler P, Fulda S, Koscielniak E, Meister MT, Scheer M, Hettmer S, Schwab M, Tremmel R, Ora I, Hutter C, Gerber NU, Lohi O, Kazanowska B, Kattamis A, Filippidou M, Goemans B, Zwaan CM, Milde T, Jager N, Wolf S, Reuss D, Sahm F, von Deimling A, Dirksen U, Freitag A, Witt R, Lichter P, Kopp-Schneider A, Jones DTW, Molenaar JJ, Capper D, Pfister SM, Witt O. The Pediatric Precision Oncology INFORM Registry: Clinical Outcome and Benefit for Patients with Very High-Evidence Targets. Cancer Discov 2021; 11: 2764-79.

Vasciaveo A, Arriaga JM, Nunes de Almeida F, Zou M, Douglass EF, Picech F, Shibata M, Rodriguez-Calero A, de Brot S, Mitrofanova A, Chua CW, Karan C, Realubit R, Pampou S, Kim JY, Afari SN, Mukhammadov T, Zanella L, Corey E, Alvarez MJ, Rubin MA, Shen MM, Califano A, Abate-Shen C. OncoLoop: A network-based precision cancer medicine framework. Cancer Discov 2022; 13 (2): 386-409.

Vercruysse T, De Bie J, Neggers JE, Jacquemyn M, Vanstreels E, Schmid-Burgk JL, Hornung V, Baloglu E, Landesman Y, Senapedis W, Shacham S, Dagklis A, Cools J, Daelemans D. The Second-Generation Exportin-1 Inhibitor KPT-8602 Demonstrates Potent Activity against Acute Lymphoblastic Leukemia. Clin Cancer Res 2017; 23: 2528-41.

Vick B, Rothenberg M, Sandhofer N, Carlet M, Finkenzeller C, Krupka C, Grunert M, Trumpp A, Corbacioglu S, Ebinger M, Andre MC, Hiddemann W, Schneider S, Subklewe M, Metzeler KH, Spiekermann K, Jeremias I. An advanced preclinical mouse model for acute myeloid leukemia using patients' cells of various genetic subgroups and in vivo bioluminescence imaging. PLoS One 2015; 10: e0120925.

Wander P, Arentsen-Peters S, Vrenken KS, Pinhanços SM, Koopmans B, Dolman MEM, Jones L, Garrido Castro P, Schneider P, Kerstjens M, Molenaar JJ, Pieters R, Zwaan CM, Stam RW. High-Throughput Drug Library Screening in Primary KMT2A-Rearranged Infant ALL Cells Favors the Identification of Drug Candidates That Activate P53 Signaling. Biomedicines 2022; 10 (3) 638.

Wang H, Guo M, Wei H, Chen Y. Targeting MCL-1 in cancer: current status and perspectives. J Hematol Oncol 2021; 14: 67.

Wang JC, Dick JE. Cancer stem cells: lessons from leukemia. Trends Cell Biol 2005; 15: 494-501.

Wang W, Sordat B, Piguet D, Sordat M. Human Colon Tumors in Nude Mice: Implantation Site and Expression of the Invasive Phenotype 1. 1982: 239-45.

Weber K, Thomaschewski M, Warlich M, Volz T, Cornils K, Niebuhr B, Tager M, Lutgehetmann M, Pollok JM, Stocking C, Dandri M, Benten D, Fehse B. RGB marking facilitates multicolor clonal cell tracking. Nat Med 2011; 17: 504-9.

Wirth AK, Wange L, Vosberg S, Henrich KO, Rausch C, Ozdemir E, Zeller CM, Richter D, Feuchtinger T, Kaller M, Hermeking H, Greif PA, Senft D, Jurinovic V, Bahrami E, Jayavelu AK, Westermann F, Mann M, Enard W, Herold T, Jeremias I. In vivo PDX CRISPR/Cas9 screens reveal mutual therapeutic targets to overcome heterogeneous acquired chemo-resistance. Leukemia 2022; 36: 2863-2874.

Wolach O, Stone RM. How I treat mixed-phenotype acute leukemia. Blood 2015; 125: 2477-85.
Wong M, Mayoh C, Lau LMS, Khuong-Quang DA, Pinese M, Kumar A, Barahona P, Wilkie EE, Sullivan P, Bowen-James R, Syed M, Martincorena I, Abascal F, Sherstyuk A, Bolanos NA, Baber J, Priestley P, Dolman MEM, Fleuren EDG, Gauthier ME, Mould EVA, Gayevskiy V, Gifford AJ,

Grebert-Wade D, Strong PA, Manouvrier E, Warby M, Thomas DM, Kirk J, Tucker K, O'Brien T, Alvaro F, McCowage GB, Dalla-Pozza L, Gottardo NG, Tapp H, Wood P, Khaw SL, Hansford JR, Moore AS, Norris MD, Trahair TN, Lock RB, Tyrrell V, Haber M, Marshall GM, Ziegler DS, Ekert PG, Cowley MJ. Whole genome, transcriptome and methylome profiling enhances actionable target discovery in high-risk pediatric cancer. Nat Med 2020; 26: 1742-53.

Worst BC, van Tilburg CM, Balasubramanian GP, Fiesel P, Witt R, Freitag A, Boudalil M, Previti C, Wolf S, Schmidt S, Chotewutmontri S, Bewerunge-Hudler M, Schick M, Schlesner M, Hutter B, Taylor L, Borst T, Sutter C, Bartram CR, Milde T, Pfaff E, Kulozik AE, von Stackelberg A, Meisel R, Borkhardt A, Reinhardt D, Klusmann JH, Fleischhack G, Tippelt S, Dirksen U, Jurgens H, Kramm CM, von Bueren AO, Westermann F, Fischer M, Burkhardt B, Wossmann W, Nathrath M, Bielack SS, Fruhwald MC, Fulda S, Klingebiel T, Koscielniak E, Schwab M, Tremmel R, Driever PH, Schulte JH, Brors B, von Deimling A, Lichter P, Eggert A, Capper D, Pfister SM, Jones DT, Witt O. Next-generation personalised medicine for high-risk paediatric cancer patients - The INFORM pilot study. Eur J Cancer 2016; 65: 91-101.

Yong KSM, Her Z, Chen Q. Humanized Mice as Unique Tools for Human-Specific Studies. Arch Immunol Ther Exp (Warsz) 2018; 66: 245-66.

Zeller C, Richter D, Jurinovic V, Valtierra-Gutierrez IA, Jayavelu AK, Mann M, Bagnoli JW, Hellmann I, Herold T, Enard W, Vick B, Jeremias I. Adverse stem cell clones within a single patient's tumor predict clinical outcome in AML patients. J Hematol Oncol 2022; 15: 25.

Zhong L, Li Y, Xiong L, Wang W, Wu M, Yuan T, Yang W, Tian C, Miao Z, Wang T, Yang S. Small molecules in targeted cancer therapy: advances, challenges, and future perspectives. Signal Transduct Target Ther 2021; 6: 201.

Links

https://www.kompetenznetz-leukaemie.de/content/patienten/leukaemien/all/ 19.10.2022; 23.10.2022

https://www.cancer.gov/types/leukemia/patient/adult-all-treatment-pdq 17.12.2022

https://www.cancer.gov/types/leukemia/patient/child-all-treatment-pdq 17.12.2022

https://www.bf3r.de/de/verwendung_von_versuchstieren_im_jahr_2020-288932.html 20.10.2022

https://pubchem.ncbi.nlm.nih.gov/gene/7514 July 2022

https://www.fda.gov/drugs/resources-information-approved-drugs/fda-grants-regular-approval-venetoclax-combination-untreated-acute-myeloid-leukemia December 2022

https://clinicaltrials.gov/ct2/results?cond=acute+leukemia&term=venetoclax&cntry=&state=&city=&dist= 16.12.2022

https://www.fda.gov/drugs/resources-information-approved-drugs/fda-approves-inotuzumab-ozogamicin-relapsed-or-refractory-b-cell-precursor-all December 2022

https://www.fda.gov/drugs/resources-information-approved-drugs/fda-grants-regular-approval-blinatumomab-and-expands-indication-include-philadelphia-chromosome December 2022

https://ncithesaurus.nci.nih.gov/ncitbrowser/ConceptReport.jsp?dictionary=NCI_Thesaurus&ns=ncit&code=C103147 25.02.23

https://www.rxabbvie.com/pdf/venclexta.pdf 25.02.23

https://www.venclexta.com/aml/taking-venclexta/dosing-schedule 26.02.23

Danksagung

Als erstes möchte ich mich bei Prof. Irmela Jeremias bedanken, die mir die Möglichkeit gegeben hat, in ihrem Labor meine Promotion zu absolvieren. Danke für dein Vertrauen, das Projekt mitgestalten zu dürfen.

Außerdem möchte ich Prof. Eckhard Wolf für die Betreuung meiner Dissertation als Doktorvater, sowie die Vertretung an der Tiermedizinischen Fakultät der Universität München danken. Vielen Dank auch an Dr. Markus Brielmeier und Dr. Binje Vick, die ebenfalls Teil meines Thesis Advisory Committees waren.

Ein großer Dank gilt an Dr. Binje Vick, meiner Betreuerin. Ich schätze es sehr wie du mich unterstützt hast. Die wissenschaftlichen Diskussionen, Feedback und unsere privaten Gespräche haben meine Zeit hier sehr geprägt. Von dir konnte ich sehr viel lernen.

Außerdem möchte ich mich bei der Arbeitsgruppe AHS bedanken für die gute Zusammenarbeit, die wissenschaftlichen Diskussionen und die schönen Momente außerhalb des Labors. Bei allen ehemaligen und aktuellen technischen Assistenten der Arbeitsgruppe möchte ich mich bedanken für die Einarbeitung und die tolle Hilfe in den letzten drei Jahren. Ein großes Dankeschön auch an ehemaligen und aktuellen Mitdoktoranden aus 002 für den ‚mental support'.

Den größten Dank widme ich meinen Eltern, Mark Frank Stanley Hunt und Petra Hunt, die mir das Studium der Tiermedizin und die Promotion in München ermöglicht haben. Ich bin euch unendlich dankbar für eure Unterstützung. Außerdem möchte ich meinen beiden Brüdern Sebastian und Christian Hunt danken.

I would also like to thank my family. You are a very special. I would also like to thank Derek ‚Bamby' Hunt, Catherine Hunt and June Kirby who were able to witness the start of this PhD and with whom I would have loved to share this moment.